

Hyperbolic band theory

Joseph Maciejko^{1,*} and Steven Rayan^{2,†}

¹*Department of Physics & Theoretical Physics Institute (TPI),
University of Alberta, Edmonton, Alberta T6G 2E1, Canada*

²*Department of Mathematics and Statistics
& Centre for Quantum Topology and Its Applications (quanTA),
University of Saskatchewan, Saskatoon, Saskatchewan S7N 5E6, Canada*

(Dated: April 2, 2024)

Abstract

Motivated by the recent realization of hyperbolic lattices in circuit quantum electrodynamics, we exploit ideas from Riemann surface theory and algebraic geometry to construct the first generalization of Bloch band theory to hyperbolic lattices, which can be formulated despite the absence of commutative translation symmetries. For an arbitrary Hamiltonian with the symmetry of a $\{4g, 4g\}$ tessellation of the hyperbolic plane, we produce a continuous family of eigenstates that acquire Bloch-like phase factors under the Fuchsian group of the tessellation, which is discrete but noncommutative. Quasi-periodic Bloch wavefunctions are then generalized to automorphic functions. Naturally associated with the Fuchsian group is a compact Riemann surface of genus $g \geq 2$, arising from the pairwise identification of sides of a unit cell given by a hyperbolic $4g$ -gon. A hyperbolic analog of crystal momentum continuously parametrizes a discrete set of energy bands and lives in a $2g$ -dimensional torus, which is a maximal set of independent Aharonov-Bohm phases threading the $2g$ noncontractible cycles of the Riemann surface. This torus is known in algebraic geometry as the Jacobian of the Riemann surface. We propose the Abel-Jacobi map — which associates to each point of the Riemann surface a point in the Jacobian — as a hyperbolic analog of particle-wave duality. Point-group symmetries form a finite group of automorphisms or self-maps of the Riemann surface and act nontrivially on the Jacobian. The tight-binding approximation and Wannier functions are also suitably generalized. In genus 1, our theory reduces to known band theory for 2-dimensional Euclidean lattices. We demonstrate our theory by explicitly computing hyperbolic Bloch wavefunctions and bandstructures numerically for a regular $\{8, 8\}$ tessellation associated with a particular Riemann surface of genus 2, the Bolza surface.

* maciejko@ualberta.ca

† rayan@math.usask.ca

I. INTRODUCTION

The concept of *Bloch wave* is a cornerstone of modern physics. Introduced by Felix Bloch in 1928 to describe the quantum-mechanical propagation of electrons in crystalline solids [1], this phenomenon applies generally to the propagation of waves of any kind in periodic media, including atomic matter waves in optical lattices, light in photonic crystals, and sound in acoustic metamaterials. The key condition for the existence of a Bloch wave is periodicity of the underlying medium — specifically, that the latter be composed of identical unit cells that are repeated under elementary translations. A Bloch wave traveling through such a medium is not itself a periodic function, but acquires predictable phase shifts under those elementary translations. The phase shifts, in turn, define the crystal momentum \mathbf{k} of the wave and its associated reciprocal space [2]. Because the allowed translations are discrete, the crystal momentum is itself a periodic variable, and an irreducible set of inequivalent crystal momenta is given by the (first) Brillouin zone. This basic fact is the foundation upon which the edifice of band theory is built [3]. Energy levels are organized into energy bands, a discrete set $\{E_n(\mathbf{k})\}$ of continuous functions of \mathbf{k} over the Brillouin zone. In d spatial dimensions, the latter is topologically equivalent to a d -dimensional torus. Our focus is on $d = 2$ spatial dimensions, where this topological space is an ordinary torus, homeomorphic to the surface of a doughnut. The nontrivial topology of the Brillouin zone, stemming from the periodicity of crystalline lattices, is ultimately responsible for the topological revolution in condensed matter physics, initiated by Haldane’s discovery of the Chern insulator [4] and firmly established through the development of a comprehensive topological band theory [5].

The absence of periodicity, that is, of a discrete translation symmetry in the system’s underlying Hamiltonian, significantly complicates the theoretical study of wave propagation. In a limited number of cases, band theory may still serve as a starting point. Localized or weak deviations from strict periodicity can often be successfully modeled as perturbations of a periodic Hamiltonian, as in standard theories of impurity states or randomized impurity scattering in crystals [3]. Incommensurate modulated phases and quasicrystals, while strongly aperiodic, can be described as projections of ordinary periodic lattices in higher dimensions [6]. Key aspects of wave propagation in such media, such as the existence of sharp Bragg peaks in x-ray diffraction, can thus be understood via analogous projections of a correspondingly higher-dimensional reciprocal space [7]. In spite of these cases, the central tenets of band theory — crystal momentum, the toroidal Brillouin zone, and sharply-defined energy bands — are expected to fundamentally break down in generic aperiodic media.

Recently, an example of a new class of synthetic aperiodic structures has been engineered using the technology of circuit quantum electrodynamics [8]. The structure is an ordered but aperiodic network of microwave resonators that, from the point of view of wave propagation, can be described effectively as a regular heptagonal tessellation of the hyperbolic plane. Such tessellations, also known as hyperbolic tilings, were studied by Coxeter [9] and popularized through M. C. Escher’s now famous “Circle Limit” woodcuts [10]. As with an ordinary two-dimensional crystal such as

graphene, whose geometry corresponds to a regular tiling of the Euclidean plane, a hyperbolic tiling consists of repeated unit cells that are all geometrically identical, but allows for patterns impossible in Euclidean space, such as a tiling by regular heptagons [8]. That such a tiling is only possible in hyperbolic space follows from the fact that the latter is endowed with a uniform negative curvature. As a result, the sum of the interior angles of an n -sided polygon is strictly less than $(n - 2)\pi$, and repeated unit cells are identical in the sense of non-Euclidean geometry. Put somewhat differently, using the phrase *geometrically identical* to describe the unit cells depends crucially upon comparing them under the lens of a particular choice of metric, the *hyperbolic* or *Poincaré* metric. As such, hyperbolic tilings are also qualitatively distinct from quasicrystalline ones, which tile the Euclidean plane (albeit aperiodically) and in which the unit cells are identical under the standard Euclidean metric. In the experiments of Ref. [8], negative curvature is simulated by artificially engineering the couplings between the resonators, such that resonators that appear closer together from a Euclidean vantage point — near the circular edge of Escher’s artwork [10], metaphorically speaking — are in fact coupled with the same strength as resonators near the center of the device, which appear further apart.

Spurred by this experimental breakthrough, recent theoretical studies have explored the propagation of matter waves on hyperbolic lattices. Using graph theory and numerical diagonalization, Ref. [11] obtained general mathematical results concerning the existence of extended degeneracies and gaps in the spectrum of tight-binding Hamiltonians on a variety of discrete hyperbolic lattices. Ref. [12] developed a hyperbolic analog of the effective-mass approximation in solid-state physics, showing that such tight-binding Hamiltonians reduce in the long-distance limit to the hyperbolic Laplacian — the Laplace-Beltrami operator associated with the Poincaré metric on the hyperbolic plane — and proposing the synthetic structures of Ref. [8] as a new platform for the simulation of quantum field theory in curved space. Topological quantum phenomena in hyperbolic lattices were explored using real-space numerical diagonalization in Ref. [13]. Notwithstanding these significant advances, quoting Ref. [8]: “no hyperbolic equivalent of Bloch theory currently exists, and there is no known general procedure for calculating band structures in either the nearly-free-electron or tight-binding limits.” The authors have thus concluded that explicit spectra can only be obtained using numerical diagonalization, “a brute-force method which yields a list of eigenvectors and eigenvalues, but no classification of eigenstates by a momentum quantum number” [8].

In this work, we present the first hyperbolic generalization of Bloch theory. We show that aperiodic Hamiltonians with the symmetry of a particular class of hyperbolic tilings can be described by such a generalization, which we dub *hyperbolic band theory*. Despite the absence of a commutative, discrete translation group, we show that a *hyperbolic crystal momentum* \mathbf{k} can be suitably defined, but lives in a vector space of dimension higher than two. There exists a corresponding *hyperbolic Brillouin zone* that is topologically equivalent to a higher-dimensional, compact torus. A *hyperbolic bandstructure* $\{E_n(\mathbf{k})\}$, a discrete set of continuous functions of \mathbf{k} on this higher-dimensional Brillouin zone, can be defined and explicitly computed.

The higher-dimensional torus that is the hyperbolic Brillouin zone is related to the tessellation

of the two-dimensional hyperbolic plane through a particular construction commonly studied in the field of algebraic geometry in mathematics. It emerges naturally from our setup that the torus always has even dimension $2g$, where g is the genus, or number of holes, of a compact Riemann surface. The torus and the Riemann surface are related by the fact that the Brillouin zone is precisely the *Jacobian* [14] of the surface. The Riemann surface is itself a minimal representation of the original configuration space, arising after quotienting the hyperbolic plane by a noncommutative translation group Γ , called a *Fuchsian group*, which amounts to identifying pairs of edges of a $4g$ -sided fundamental cell — see [Fig. 1(c)].

The so-called Jacobian is a geometric object that is naturally associated to every Riemann surface and plays the role of storing a complete geometric record of the distinct $U(1)$ -representations of the fundamental group of the Riemann surface. For instance, when we tile the hyperbolic plane with Poincaré-regular octagons, then the Riemann surface has genus 2 and the Brillouin zone is a 4-dimensional torus. This example will be crucial for us in illustrating the theory.

From the point of view of the presence of Riemann surfaces, our hyperbolic band theory is simultaneously a *higher-genus band theory*. In comparison, ordinary band theory is a genus-one theory, where the now standard two-dimensional torus arises as the quotient of the Euclidean plane by a commutative, discrete group of lattice translations, where the lattice is determined by a (4×1) -sided fundamental cell. The torus serves both as a minimal representation of the configuration space and as reduced momentum space. Viewed from algebraic geometry, the real space torus is a genus-one Riemann surface known commonly as an *elliptic curve* and the momentum space torus is the Jacobian of the elliptic curve. Indeed, it is a classical fact from algebraic geometry that an elliptic curve and its Jacobian are isomorphic, not only topologically but also as complex manifolds. The equivalence between them is given by the Abel-Jacobi map [14], which can be thought of as a geometric Fourier transform. Because of their identical geometry, one can pass easily back and forth between the two tori, blurring the lines between position space and momentum space when convenient. In our hyperbolic band theory, the Riemann surface and the Jacobian no longer share the same topology, nor even the same dimension. Still, the passage between them is given by a higher-dimensional Abel-Jacobi map, which can be approximated numerically as required. The realization of the role of algebraic geometry in what has been, until now, a squarely topological theory of materials anticipates a plethora of new constructions and algebro-geometric invariants for describing and classifying quantum material structures.

For the benefit of the reader, we summarize here the essence of our construction, review the necessary elements of hyperbolic and algebraic geometry, and provide detailed derivations in subsequent sections. We specifically consider regular tilings described by the Schläfli symbol $\{4g, 4g\}$, with $g \geq 2$ an integer, which are necessarily hyperbolic. These can be viewed as lattices in which the repeated unit cell is a hyperbolic $4g$ -gon, $4g$ of which meet at each vertex of the lattice. While aperiodic, such lattices admit the analog of a discrete translation group — this is the discrete, noncommutative Fuchsian group Γ , which is naturally a subgroup of the isometry group $SL(2, \mathbb{R})$ of the hyperbolic plane [15]. Under the correct conditions, the quotient of the hyperbolic plane

by Γ is the aforementioned compact Riemann surface of genus g . In ordinary Bloch theory, the two components k_x and k_y of the crystal momentum can be interpreted as Aharonov-Bohm fluxes threading the two distinct noncontractible cycles of this “compactified unit cell”. In the hyperbolic case, a Riemann surface of genus g possesses $2g$ noncontractible cycles; thus a $2g$ -dimensional hyperbolic crystal momentum \mathbf{k} can be defined, whose components correspond to Aharonov-Bohm fluxes through the $2g$ noncontractible cycles of the compactified $4g$ -gonal unit cell. (In an entirely different context, fluxes of this type are responsible for the protected ground-state degeneracy of topologically ordered states, such as fractional quantum Hall states and gapped spin liquids, on higher-genus Riemann surfaces [16].) In conventional band theory, the bandstructure is obtained by diagonalizing the Hamiltonian on a single unit cell, with periodic boundary conditions “twisted” by the two Aharonov-Bohm fluxes k_x and k_y [3]. Since the corresponding eigenvalue problem is Hermitian, and the solution domain compact, a discrete set of real eigenvalues $\{E_n(\mathbf{k})\}$ is obtained for each \mathbf{k} , producing the bandstructure. The hyperbolic bandstructure is obtained analogously here by diagonalizing the Hamiltonian on a single hyperbolic $4g$ -gon with “periodic” boundary conditions twisted by the $2g$ components of the hyperbolic crystal momentum \mathbf{k} . Provided the resulting eigenvalue problem is Hermitian, a discrete set of real eigenvalues for each \mathbf{k} is again obtained: the hyperbolic bandstructure $\{E_n(\mathbf{k})\}$ over the Jacobian torus. The corresponding *hyperbolic Bloch eigenstates* $\psi_{\mathbf{k}}$ are automorphic functions on the hyperbolic plane [17], generalizations of (quasi-)periodic functions on the Euclidean plane, which acquire a \mathbf{k} -dependent phase factor under noncommutative Γ -translations.

II. HYPERBOLIC LATTICES AND FUCHSIAN GROUPS

A. Preliminaries

In the absence of a periodic potential, the propagation of electrons on the two-dimensional (2D) Euclidean plane $\mathbb{E} \cong \mathbb{R}^2$ is described by the usual free-particle Hamiltonian

$$H_0 = \frac{\mathbf{p}^2}{2m} = -\frac{\nabla^2}{2m}, \quad (1)$$

where m is the electron mass and $\mathbf{p} = -i\nabla$ is the momentum operator. The continuous translation invariance of H_0 is expressed mathematically by the fact that it commutes with the operator $T_{\mathbf{a}} = e^{-i\mathbf{p}\cdot\mathbf{a}}$ for translations of \mathbb{E} by an arbitrary vector \mathbf{a} . Likewise, its continuous $SO(2)$ symmetry under planar rotations corresponds to the fact that $[H_0, R(\theta)] = 0$, where $R(\theta) = e^{-i\theta L_z}$ is the rotation operator through angle θ , with $L_z = -i\partial/\partial\theta$ the angular momentum operator. Together, translations and rotations form the special Euclidean group $SE(2)$ of rigid motions of \mathbb{E} .

The Hamiltonian of an electron propagating freely in the 2D hyperbolic plane \mathbb{H} should therefore likewise also be invariant under the group of rigid motions of this space, which is the projective special linear group $PSL(2, \mathbb{R}) \cong SL(2, \mathbb{R})/\{\pm I\}$, consisting of unimodular 2×2 real matrices

modulo multiplication by an overall sign [18]. We will be mostly working with the Poincaré disk model of the hyperbolic plane, in which \mathbb{H} corresponds to the interior of the complex unit disk $|z| < 1$, with the Poincaré metric given in line element form by

$$ds^2 = \frac{4(dx^2 + dy^2)}{(1 - |z|^2)^2}, \quad (2)$$

with $z = x + iy$. The Poincaré disk model also underlies the effectively non-Euclidean geometry of the engineered structures in Ref. [8]. In this model, an element γ of $PSL(2, \mathbb{R})$ is represented more conveniently as an element of the isomorphic group $PSU(1, 1) \cong SU(1, 1)/\{\pm I\}$, where

$$SU(1, 1) = \left\{ \gamma = \begin{pmatrix} \alpha & \beta \\ \beta^* & \alpha^* \end{pmatrix} : \alpha, \beta \in \mathbb{C}, |\alpha|^2 - |\beta|^2 = 1 \right\}, \quad (3)$$

and acts on a point $z \in \mathbb{H}$ by linear fractional transformations, which are the classical Möbius transformations:

$$z \rightarrow \gamma(z) = \frac{\alpha z + \beta}{\beta^* z + \alpha^*}. \quad (4)$$

Since the Euclidean free-particle Hamiltonian H_0 is proportional to the Euclidean Laplacian ∇^2 , its natural generalization to the hyperbolic case is

$$H_0 = -\Delta, \quad (5)$$

where

$$\Delta = \frac{1}{4}(1 - |z|^2)^2 \left(\frac{\partial^2}{\partial x^2} + \frac{\partial^2}{\partial y^2} \right), \quad (6)$$

is the Laplace-Beltrami operator on the Poincaré disk \mathbb{H} , which we will refer to as the hyperbolic Laplacian. One explicitly checks that (5) commutes with the $PSL(2, \mathbb{R})$ transformations (4).

B. Periodic potentials on a Euclidean lattice and Bloch phases

To understand the consequences of introducing a potential $V(x, y)$ compatible with a hyperbolic tessellation, it will be helpful to spend a few moments recalling the story from the Euclidean case. Here, the Hamiltonian is augmented as $H = H_0 + V$ and is now only invariant under a discrete subgroup $G \subset SE(2)$. We shall take the potential to have the symmetry of a square lattice [Fig. 1(a)], with the lattice constant set to unity. As Bloch's theorem is a consequence of the periodicity of H exclusively [3], we will ignore point-group operations and take G to be the abelian group of discrete translations on the lattice. The latter is isomorphic as a group to $\mathbb{Z} \times \mathbb{Z}$ and is generated by two elementary translations, $T_x : (x, y) \rightarrow (x + 1, y)$ and $T_y : (x, y) \rightarrow (x, y + 1)$ for the square lattice. Bloch's theorem states that eigenstates of H have the property

$$\psi(x + 1, y) = e^{ik_x} \psi(x, y), \quad \psi(x, y + 1) = e^{ik_y} \psi(x, y). \quad (7)$$

Since k_x and k_y appear as phase factors, they are only determined up to integer multiples of 2π ; thus, $\mathbf{k} = (k_x, k_y)$ lives in the first Brillouin zone $[-\pi, \pi] \times [-\pi, \pi] / \sim$, where \sim is the antipodal map that identifies $\pm\pi$ in each summand. The resulting space of phase factors is of course homeomorphic to a 2-torus $T^2 = (S^1)^2$.

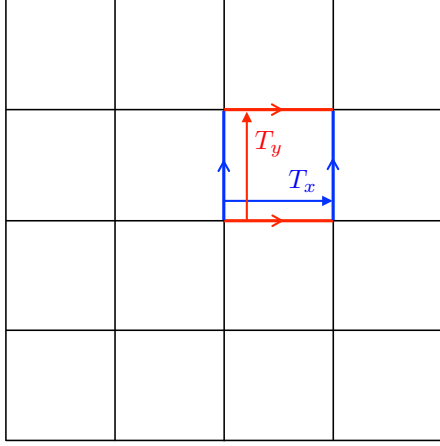
Eigenfunctions of H satisfying the Bloch condition can be explicitly constructed as follows. One solves the Schrödinger equation in a reference unit cell \mathcal{D} , say $[0, 1] \times [0, 1]$, with the twisted, periodic boundary conditions

$$\psi(1, y) = e^{ik_x} \psi(0, y), \quad \psi(x, 1) = e^{ik_y} \psi(x, 0), \quad (8)$$

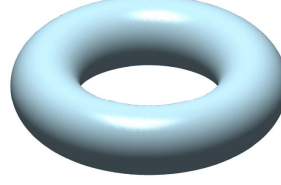
and identical conditions on $\partial_x \psi$ and $\partial_y \psi$, obtained by taking derivatives of the Bloch condition (7). Since the unit cell is a compact region and the Hamiltonian is self-adjoint on the space of twice-differentiable, square-integrable functions $\mathcal{L}^2(\mathcal{D})$ with such boundary conditions, one obtains a discrete set of real eigenvalues $E_n(\mathbf{k})$ for H on \mathcal{D} . Since H is the same in every unit cell, the corresponding solution on the entire Euclidean plane \mathbb{E} is simply obtained by translating the solution in \mathcal{D} in a manner that respects the Bloch condition (7). The solution at position $\mathbf{r} = (x, y)$ in a unit cell displaced from \mathcal{D} by the lattice translation $\mathbf{R} = (R_x, R_y) \in \mathbb{Z}^2$ is given in terms of the solution in \mathcal{D} by $\psi(\mathbf{r}) = e^{i\mathbf{k} \cdot \mathbf{R}} \psi(\mathbf{r} - \mathbf{R})$. This function obeys the Schrödinger equation and the Bloch condition everywhere, and the function and its derivatives are manifestly continuous.

To generalize the ideas at play to the hyperbolic case, it will be useful to reinterpret this manner of constructing Bloch waves for H as follows. In reducing the Schrödinger problem on \mathbb{E} to its solution on a single unit cell \mathcal{D} , we replace \mathbb{E} with its quotient by G . This action produces a 2-torus: $\mathbb{E}/G \cong \mathbb{R}^2/\mathbb{Z}^2 \cong T^2$ [Fig. 1(b)]. The phase factors e^{ik_x} and e^{ik_y} in Eq. (7) can then be interpreted as Aharonov-Bohm phases produced by fluxes, $k_x = \oint_{C_x} A$ and $k_y = \oint_{C_y} A$, which thread the two noncontractible cycles C_x, C_y of this torus, where A is a flat connection on the torus. Alternatively, each Bloch phase factor can be viewed as a $U(1)$ -representation of the fundamental group of the torus, $\pi_1(T^2)$, which is generated by the homotopy classes C_x and C_y and obeys the presentation $C_x C_y C_x^{-1} C_y^{-1} = 1$ [19]. The representation $\chi(C_{x,y}) = \chi(C_{x,y}^{-1})^* = e^{ik_{x,y}} \in U(1)$ manifestly obeys this presentation. Note that $\pi_1(T^2) \cong \mathbb{Z}^2$ is in fact isomorphic to G . Thus, we recover the usual point of view according to which the Bloch phase factors form a $U(1)$ -representation of the discrete translation group.

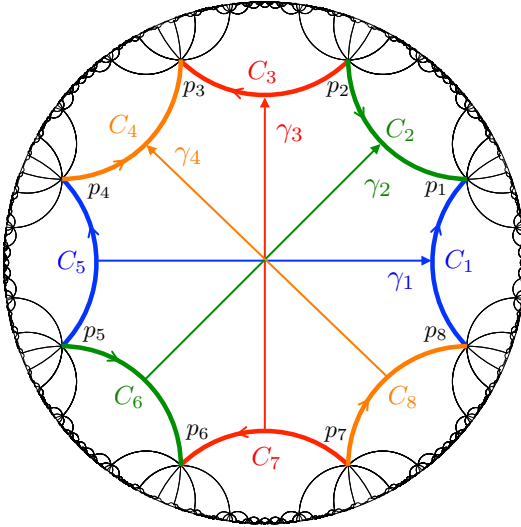
What may be overlooked is that, strictly speaking, the construction above involves *two* homeomorphic 2-tori. The first, which we shall denote Σ , is the one obtained by taking the real configuration space \mathbb{E} and quotienting by the symmetry group of the lattice. The second, which we shall call the *Jacobian* of Σ and denote $\text{Jac}(\Sigma)$, is obtained from collecting the Bloch phase factors into a topological space, which naturally has the topology of $T^2 = (S^1)^2$. In fact, we take as a definition that $\text{Jac}(\Sigma)$ is the set of all representations of $\pi_1(\Sigma)$ into $U(1)$, although classically there are several distinct-appearing yet equivalent ways to define the Jacobian [14]. It is also crucial to observe that these two spaces are not simply topological tori but rather complex manifolds. The torus Σ was constructed from the choice of the translations T_x and T_y , which correspond to



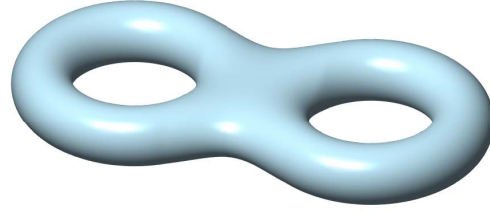
(a)



(b)



(c)



(d)

FIG. 1. For the Euclidean lattice (a), the translations T_x, T_y identify pairwise the four sides of the unit cell, which gives the ordinary torus (b). On the hyperbolic lattice (c), Fuchsian group transformations $\gamma_1, \gamma_2, \gamma_3, \gamma_4$ identify pairwise the eight sides of the hyperbolic unit cell, which gives the genus-2 surface (d). In both (a) and (c), the identifications preserve the orientations of the sides, which are indicated by arrows.

the basis vectors 1 on the real axis and i on the imaginary one. Their ratio $\tau = i/1 = i$ is the value of a parameter in the complex upper half-plane that determines a particular *elliptic curve*, which is a compact Riemann surface of genus 1. The Riemann surface structure is extra geometric information on top of the topological structure of the torus. At the same time, the choice of τ determines a particular elliptic curve structure on $\text{Jac}(\Sigma)$, which we can take to be identical to that of Σ . In general, there is no canonical choice of identification between an elliptic curve and

its Jacobian. Any such identification depends upon a choice of base point, which is the basepoint for the Abel-Jacobi map, and changes of basepoint are simply translations of the lattice. We will revisit this explicitly in Sec. IID. Another interesting observation is that both Σ and $\text{Jac}(\Sigma)$ are algebraic groups, as elliptic curves come equipped with an abelian group law, the existence of which has tremendous implications for number theory and cryptography (e.g., Ref. [20]). On the Jacobian side, the group structure manifests in the addition of crystal momenta, $\mathbf{k} + \mathbf{k}'$, modulo a reciprocal lattice vector.

C. Automorphic potentials on a hyperbolic tessellation and hyperbolic Bloch phases

We now turn to the hyperbolic case, where we consider a potential $V(x, y)$ with the symmetry of a $\{4g, 4g\}$ hyperbolic tiling with $g \geq 2$. We first outline the key steps of our construction for general tilings of this type, and later proceed with detailed calculations for a specific example: the Poincaré regular octagonal $\{8, 8\}$ tiling ($g = 2$) illustrated in [Fig. 1(c)].

The general Hamiltonian $H = H_0 + V$ — with H_0 given in Eq. (5) — is invariant not under continuous $PSL(2, \mathbb{R})$ transformations, but rather under the discrete Fuchsian group $\Gamma \subset PSL(2, \mathbb{R})$ associated with the tiling. While nonabelian in general, this group behaves as a hyperbolic analog of a discrete translation group: it acts properly discontinuously on the hyperbolic plane \mathbb{H} , meaning that its repeated action on a single fundamental region or reference unit cell \mathcal{D} in \mathbb{H} tiles all of \mathbb{H} with geometrically identical copies of \mathcal{D} , with neither gaps nor overlaps [15]. We will focus on the case where Γ is co-compact and strictly hyperbolic, in which case the unit cell \mathcal{D} is compact and has finite area under the Poincaré metric (2). For the $\{4g, 4g\}$ tiling, \mathcal{D} is a hyperbolic $4g$ -gon, meaning a polygon whose $4g$ sides are geodesic segments under the metric. The uniformization theorem, an important result appearing in algebraic geometry, differential geometry, and number theory, states that the quotient \mathbb{H}/Γ is a smooth, compact Riemann surface Σ_g of genus $g \geq 2$. Topologically, this surface originates from $2g$ pairwise identifications of the sides of \mathcal{D} under the action of Γ . Such a surface has $2g$ noncontractible cycles, corresponding to homotopy classes $a_1, b_1, \dots, a_g, b_g$ through a common basepoint $p_0 \in \Sigma_g$ and through which $2g$ Aharonov-Bohm fluxes $k_a^{(1)}, k_b^{(1)}, \dots, k_a^{(g)}, k_b^{(g)} \in [0, 2\pi)$ can be threaded. These can be interpreted again as arising from a flat connection A on Σ_g :

$$k_a^{(i)} = \oint_{a_i} A, \quad k_b^{(i)} = \oint_{b_i} A, \quad i = 1, \dots, g. \quad (9)$$

The set of $2g$ phase factors $e^{ik_a^{(1)}}, e^{ik_b^{(1)}}, \dots, e^{ik_a^{(g)}}, e^{ik_b^{(g)}}$ forms yet again a $U(1)$ -representation χ of the fundamental group of Σ_g , which is freely generated by the homotopy classes of Σ_g , for instance:

$$\pi_1(\Sigma_g) \cong \{a_1, b_1, \dots, a_g, b_g : a_1 b_1 a_1^{-1} b_1^{-1} \dots a_g b_g a_g^{-1} b_g^{-1} = 1\}. \quad (10)$$

We define the representation $\chi : \pi_1(\Sigma_g) \rightarrow U(1)$ in terms of the Aharonov-Bohm fluxes in Eq. (9)

by

$$\chi(a_i) = \chi(a_i^{-1})^* = e^{ik_a^{(i)}}, \quad \chi(b_i) = \chi(b_i^{-1})^* = e^{ik_b^{(i)}}, \quad i = 1, \dots, g. \quad (11)$$

In analogy with the Euclidean case of Sec. II B, the Fuchsian group Γ is in fact isomorphic to $\pi_1(\Sigma_g)$ [21]. The (nonunique) choice of presentation of $\pi_1(\Sigma_g)$, an example of which is given in Eq. (10), depends on the particular action of Γ on \mathbb{H} . Isomorphic subgroups $\Gamma \subset PSL(2, \mathbb{R})$ that generate the same $\{4g, 4g\}$ hyperbolic tiling are the analog of distinct choices of basis vectors for the same periodic lattice in the Euclidean case.

In this geometric picture, we again have two complex manifolds, although they are no longer isomorphic — not as complex manifolds and not even topologically. One is the Riemann surface Σ_g , which is a minimal domain for the real configuration space. As in the Euclidean case, there is a particular complex manifold structure on Σ_g that is inherited from the quotient by Γ (and hence from the particular choice of tessellation). The other manifold is $\text{Jac}(\Sigma_g)$, the Jacobian of Σ_g which parametrizes distinct $U(1)$ -representations χ of $\pi_1(\Sigma_g)$. The manifold Σ_g is 2-dimensional over the real numbers (or 1-dimensional over \mathbb{C}) just as in the Euclidean case, although it is no longer homeomorphic to a torus. On the other hand, $\text{Jac}(\Sigma_g)$ is $2g$ -dimensional over \mathbb{R} — in fact, it is homeomorphic to the torus $T^{2g} = (S^1)^{2g}$. Yet another difference is that while $\text{Jac}(\Sigma_g)$ remains a group under addition of phases, Σ_g does not admit a group law.

From these observations, we propose that despite the absence of an abelian translation group, the choice of a $\{4g, 4g\}$ hyperbolic lattice induces naturally a notion of crystal momentum: a $2g$ -dimensional hyperbolic crystal momentum,

$$\mathbf{k} = \left(k_a^{(1)}, k_b^{(1)}, \dots, k_a^{(g)}, k_b^{(g)}\right) \in [-\pi, \pi]^{2g} / \sim \cong T^{2g} \cong \text{Jac}(\Sigma_g), \quad (12)$$

where \sim is again the antipodal map on intervals. In other words, we propose that $\text{Jac}(\Sigma_g)$ plays the role of a *hyperbolic Brillouin zone*. By analogy with the Euclidean case described earlier, the notion of hyperbolic crystal momentum can be used to construct eigenfunctions ψ of H starting from a single reference unit cell \mathcal{D} . For $z = x + iy$ in the Poincaré disk, we generalize the Bloch condition (7) to

$$\psi(\gamma(z)) = \chi(\gamma)\psi(z), \quad (13)$$

where $\gamma \in \Gamma$ acts according to Eq. (4) and where $\chi : \Gamma \rightarrow U(1)$ is some map. Appearing as early as works of Poincaré, functions obeying the condition (13) are known as *automorphic functions* with *factor of automorphy* χ [17, 22], and can be seen as hyperbolic analogs of periodic functions. The factor of automorphy here is the simplest kind possible, which is of weight 0, also known as a *multiplier system*. More generally, one may consider factors of automorphy that depend holomorphically on z — that is, weight- k factors of automorphy $\hat{\chi}(\gamma, z) = \chi(\gamma)(cz + d)^k$ for some real numbers c and d , and where $\chi : \Gamma \rightarrow U(1)$ and $z \in \mathbb{H}$. We consider only unitary automorphic factors in our Bloch condition, in reflection of the Euclidean situation.

By assumption, the potential V itself is an automorphic function with trivial automorphy factor, $V(\gamma(z)) = V(z)$. Accordingly, we shall refer to such a potential as an *automorphic potential*. Again, we solve the Schrödinger equation

$$(-\Delta + V)\psi = E\psi, \quad (14)$$

on the single reference unit cell \mathcal{D} , with the boundary conditions specified by Eq. (13). By analogy with the Euclidean or genus-1 case (7), there are now $2g$ linearly independent boundary conditions to apply, corresponding to the $2g$ generators of $\pi_1(\Sigma_g)$. In practice, one requires an explicit representation of those generators as $PSU(1, 1)$ matrices [see Eq. (3)]. The potential V does not involve derivatives and is thus trivially self-adjoint. With the boundary conditions (13), the hyperbolic Laplacian Δ can be shown to be self-adjoint on \mathcal{D} as well [23]. Since the region is compact, we obtain a discrete set of real eigenvalues $\{E_n(\mathbf{k})\}$ for each value of the hyperbolic crystal momentum \mathbf{k} in Eq. (12). Since H is the same in every unit cell, i.e., it is invariant under the action of Γ , the solution on \mathcal{D} can be extended to the entire Poincaré disk \mathbb{H} by Γ -translating it in a manner that respects the generalized Bloch condition (13). In other words, the solution in any fundamental domain $\mathcal{D}' \subset \mathbb{H}$, that is necessarily the image of \mathcal{D} under the action of a particular element $\gamma \in \Gamma$, is given by

$$\psi(z) = \chi(\gamma)\psi(\gamma^{-1}(z)), \quad (15)$$

where $z \in \mathcal{D}'$ and $\gamma^{-1}(z) \in \mathcal{D}$. This construction ensures that, as in the Euclidean case, ψ obeys the Schrödinger equation (14) and the generalized Bloch condition (13) everywhere, and ψ and its derivatives are continuous in the entire Poincaré disk. The factors of automorphy χ play the role of phase factors, and are precisely $U(1)$ -representations of $\pi_1(\Sigma_g)$ as defined in Eq. (11).

With these observations in hand, we have the desired identifications: $\text{Jac}(\Sigma_g)$ is indeed our hyperbolic momentum space and we may describe each factor of automorphy χ as a *hyperbolic Bloch phase*.

D. Hyperbolic particle-wave duality: complex geometry and the Abel-Jacobi map

The geometry emerging from our construction is a pair of complex manifolds, Σ_g and $\text{Jac}(\Sigma_g)$. In the Euclidean case, these manifolds manifest as a pair of essentially indistinguishable elliptic curves. One can ask whether we retain a direct passage from one to the other in the hyperbolic, or $g \geq 2$, case.

To this end, let us reexamine the Riemann surface Σ_g with a view to its complex manifold structure. That Σ_g is a complex manifold is the same as saying that it possesses a tensor field J that acts on the tangent spaces $T_p\Sigma_g$, $p \in \Sigma_g$, with the properties that $J^2 = -\mathbb{I}$, where \mathbb{I} is the identity, and that J is integrable in the sense of Newlander-Nirenberg [24]. The integrability condition asks that the Nijenhuis tensor of J vanishes identically [19, 24]. Note that the eigenvalues

of J can be seen as the origin of the imaginary units $\pm i$ on each tangent space. Seeing that the Fuchsian quotient \mathbb{H}/Γ always possesses an integrable complex structure J requires some careful mathematical analysis treated, for instance, in [25].

Just as topological structures lead to continuous functions and differentiable structures to smooth functions, it is natural to ask how J gives rise to *holomorphic functions* on Σ_g . The surface is equipped with a *Cauchy-Riemann operator* $\bar{\partial} = [J, D]$, where D differentiates (in the ordinary sense) functions $f : \mathbb{R}^2 \rightarrow \mathbb{R}^2$ on local patches of Σ_g . For insight, a useful toy case is to consider just a vector space $V \cong \mathbb{R}^2$ with the standard complex structure

$$J = \begin{pmatrix} 0 & -1 \\ 1 & 0 \end{pmatrix}.$$

This structure is automatically integrable as we are working over a single vector space instead of the entire collection of tangent spaces of Σ_g . (Put differently, we have replaced our Riemann surface with a single point.) Then, one can check that the commutator $[J, D]$ computes exactly the Cauchy-Riemann equations. Working over all of Σ_g , the operator $\bar{\partial}$ allows us to state what it means for a function $f : \Sigma_g \rightarrow \mathbb{R}^2 \cong \mathbb{C}$ to be holomorphic: the functions in the kernel of $\bar{\partial}$ are precisely the holomorphic ones.

Now, recall that the cotangent bundle $T^*\Sigma_g$ of our Riemann surface is a smooth vector bundle of real rank 2, meaning that the fiber is 2-dimensional over the real numbers. Its sections are precisely the one-forms on Σ_g , and the bundle is dual to the tangent bundle $T\Sigma_g$, whose sections are the vector fields. The bundle $T^*\Sigma_g$ is equipped with an additional structure, which is a natural holomorphic structure compatible with J . We can think about this as a relationship between the Cauchy-Riemann operator on Σ_g and an analogous operator on $T^*\Sigma_g$, called the Dolbeault operator, whose kernel tells us which one-forms are holomorphic. Rather than define the Dolbeault operator directly, we can simply say that the holomorphic one-forms on Σ_g are the ones that can be written locally as $\theta = f dz$, where f is a holomorphic function on Σ_g in the sense defined by J above.

Restricting to the holomorphic one-forms, we generate the *holomorphic cotangent bundle* of Σ_g , referred to frequently in algebraic geometry as the *canonical line bundle* [26]. (This bundle is a “line” bundle in the sense that, while its fibers are 2-dimensional over \mathbb{R} , we have shifted to a complex point of view and they are in fact 1-dimensional over \mathbb{C} .) A well-known result in algebraic geometry that follows from the Riemann-Roch theorem and Serre duality (e.g., [27, 28]) is that the space of global holomorphic sections of K is g -dimensional. In other words, there are g -many global, linearly independent, holomorphic one-forms $\theta_1, \dots, \theta_g$ on Σ_g . This is an algebraic interpretation of the genus that complements the topological one: rather than counting the number of holes, we think of g as counting the number of independent one-forms — a fact consistent with the reality that there is no global holomorphic one-form on the Riemann sphere other than $\theta = 0$.

Now, recall that we chose $2g$ cycles with a common basepoint p_0 via which we defined Aharonov-Bohm fluxes, leading to $U(1)$ -representations χ of $\pi_1(\Sigma_g)$. These cycles provide a basis for the

first homology group of the surface. At this point, we will replace these cycles with a *symplectic basis*, which is a collection of loops a_i, b_i , $i = 1, \dots, g$, such that a_i and b_i intersect in exactly one point and all other intersections are empty. At the same time, we choose a basis $\theta_1, \dots, \theta_g$ of holomorphic one-forms in such a way that they are “dual” to the a loops, meaning

$$\oint_{a_i} \theta_j = \delta_{ij}.$$

The remaining integrals, which form g -many g -tuples

$$\left(\oint_{b_1} \theta_j, \dots, \oint_{b_g} \theta_j \right),$$

produce a nondegenerate $g \times g$ matrix Ω , the *period matrix* of Σ_g . The full rank of Ω follows from the Riemann bilinear relations [14]. As such, the columns are a basis for \mathbb{C}^g , giving us a lattice structure on the underlying \mathbb{R}^{2g} , known as the *period lattice*. Let us denote this lattice by Λ . The quotient \mathbb{R}^{2g}/Λ is precisely $\text{Jac}(\Sigma_g)$. The matrix Ω can be shown to be always symmetric with positive-definite imaginary part. The space of all such matrices is called the *Siegel upper half-space*. Note that in the $g = 1$ or elliptic curve case, the period matrix is 1×1 — it is precisely the modular parameter τ in the upper half-plane.

Now, let p be any point in Σ_g and let c_p be an continuous path from p_0 to p , where p_0 is a basepoint (not necessarily the one we chose earlier). We can define a map $a : \Sigma_p \rightarrow \text{Jac}(\Sigma_p)$ by setting

$$a(p) = \left(\int_{c_p} \theta_1, \dots, \int_{c_p} \theta_g \right) \bmod \Lambda. \quad (16)$$

Here, the integral yields a vector in $\mathbb{C}^g \cong \mathbb{R}^{2g}$. We then translate the output to the fundamental unit cell in $\mathbb{C}^g \cong \mathbb{R}^{2g}$ of the lattice Λ , thus producing a point in $\text{Jac}(\Sigma_g)$ — equivalently, a crystal momentum \mathbf{k} . It is readily apparent that the map is independent of both the specific basepoint, as well as the chosen path to p . Changing the path perturbs the calculation by an integral over a cycle, which can be written in the basis (a_i, b_i) , and so the difference that we pick up is precisely an element of Λ . This difference is killed by the quotient. Changing the basepoint simply translates the torus. Finally, when we take $p = p_0$, we are integrating only over cycles, which again are killed by the quotient, and so $a(p_0) = \mathbf{k} = 0$ is the identity in the Jacobian as a group.

The map defined here is the Abel-Jacobi map. As it maps a 1-dimensional space (over \mathbb{C}) to a g -dimensional space, it is only an isomorphism in the genus-1 case, where it provides the familiar particle-wave duality of Euclidean quantum mechanics and, hence, conventional band theory. Intuitively, the line integrals in Eq. (16) can be interpreted as the set of topologically distinct contributions to the geometric phase accumulated under adiabatic motion of a quantum particle from a reference point p_0 to a given point p inside the unit cell. In the Euclidean case, the unit cell is geometrically flat, and the two contributions to the geometric phase are linear

functions of two linearly independent displacements, producing an isomorphism between real and momentum spaces. Apart from the obvious dimensional differences inherent in the hyperbolic case, the nontrivial negative curvature of the unit cell required by the Gauss-Bonnet theorem renders such a linear mapping impossible.

To counter the difference in dimension between the configuration and momentum spaces for $g \geq 2$, we can ask about the effect of applying the map in Eq. (16) to g -tuples of points from Σ_g . Indeed, we may consider the map

$$a(p_1, \dots, p_g) = \sum_{i=1}^g \left(\int_{c_{p_i}} \theta_1, \dots, \int_{c_{p_i}} \theta_g \right) \bmod \Lambda. \quad (17)$$

One simple observation is that the order of the g inputs has no effect on the output, and so the map is best defined not on the Cartesian product $(\Sigma_g)^g$ but rather on the symmetric product $S^g(\Sigma_g) := (\Sigma_g)^g / S_g$, where S_g is the symmetric group on g letters. It is a classical fact from algebraic geometry, e.g., [29], that this map $a : S^g(\Sigma_g) \rightarrow \text{Jac}(\Sigma_g)$ is *almost* an isomorphism of complex manifolds. The map is only *birational*, which means that a certain submanifold of $S^g(\Sigma_g)$ must be blown down in order to recover $\text{Jac}(\Sigma_g)$. This submanifold is an example of a “high-symmetry” region, related to the so-called *theta divisor* in $\text{Jac}(\Sigma_g)$ [14]. While involving some technical aspects of algebraic geometry, this construction exhibits the Jacobian as a particular complex manifold constructed from the data of our Riemann surface in a direct way, providing an algebraic particle-wave duality that exists in spite of dimensional and curvature differences.

The aforementioned high-symmetry region is worthy of further investigation, as it suggests the existence of a special set of points in the hyperbolic unit cell whose physical relevance is not yet appreciated. The map further suggests that an ideal Liouville-Arnol’d-type phase space for this physical system in which the configuration space and momentum space have equal dimension might be given by a fibration of Jacobian tori over a g -dimensional complex space associated to Σ_g . We leave the formalization of this dynamical system to forthcoming work. In the meantime, we now proceed with a concrete example of our hyperbolic band theory in genus $g = 2$.

III. THE HYPERBOLIC BLOCH PROBLEM ON THE BOLZA LATTICE

Having outlined the key ideas of our general theory, we now apply it to the simplest hyperbolic analog of the Euclidean square lattice: the regular octagonal $\{8, 8\}$ tiling depicted in [Fig. 1(c)]. This tiling is generated by the action of a Fuchsian group Γ on a reference unit cell \mathcal{D} , which can be taken to be the regular hyperbolic octagon centered at the origin $z = 0$ of the Poincaré disk, that is, the region bounded by the colored geodesic segments C_1, \dots, C_8 in [Fig. 1(c)]. These segments are circular arcs normal to the boundary at infinity $|z| = 1$, and can be parametrized as follows:

$$C_j = \left\{ z = e^{i(j-1)\frac{\pi}{4}}(c + re^{i\theta}), \frac{3\pi}{4} < \theta < \frac{5\pi}{4} \right\}, \quad j = 1, \dots, 8, \quad (18)$$

where

$$c = \sqrt{\frac{3 + 2\sqrt{2}}{2 + 2\sqrt{2}}}, \quad r = \frac{1}{\sqrt{2 + 2\sqrt{2}}}. \quad (19)$$

The vertices of \mathcal{D} are given by

$$p_j = 2^{-1/4} e^{i(2j-1)\frac{\pi}{8}}, \quad j = 1, \dots, 8. \quad (20)$$

An explicit $PSU(1, 1)$ matrix representation of the four generators $\gamma_1, \gamma_2, \gamma_3, \gamma_4$ which freely generate Γ is given in Ref. [30]:

$$\gamma_j = \begin{pmatrix} 1 + \sqrt{2} & (2 + \sqrt{2})\lambda e^{i(j-1)\pi/4} \\ (2 + \sqrt{2})\lambda e^{-i(j-1)\pi/4} & 1 + \sqrt{2} \end{pmatrix}, \quad j = 1, \dots, 4, \quad (21)$$

where $\lambda = \sqrt{\sqrt{2} - 1}$. One can check by explicit computation that the action of those generators identifies the boundary segments pairwise and in an orientation-preserving manner, as depicted in Fig. 1(c):

$$\gamma_1(C_5) = C_1, \quad \gamma_2(C_6) = C_2, \quad \gamma_3(C_7) = C_3, \quad \gamma_4(C_8) = C_4. \quad (22)$$

The inverse Möbius transformations γ_j^{-1} correspond simply to the matrix inverse of Eq. (21). The generators of Γ obey the relation

$$\gamma_1 \gamma_2^{-1} \gamma_3 \gamma_4^{-1} \gamma_1^{-1} \gamma_2 \gamma_3^{-1} \gamma_4 = \mathbb{I}, \quad (23)$$

where \mathbb{I} again denotes the identity. As shown in Appendix A, Eq. (23) is precisely the presentation of the fundamental group $\pi_1(\Sigma_2)$ of a smooth, compact genus-2 surface, illustrated schematically in [Fig. 1(d)], that is obtained by gluing together the opposite sides of the hyperbolic octagon \mathcal{D} . This establishes the group isomorphism $\pi_1(\Sigma_2) \cong \Gamma$. We emphasize that while all genus-2 topological surfaces share this fundamental group, the symbol Σ_2 refers not to *any* genus-2 surface but specifically to the quotient \mathbb{H}/Γ for the Γ generated above. This quotient is precisely the side identification illustrated in [Fig. 1(c)]. To use our earlier language, Σ_2 is a particular Riemann surface structure defined upon a topological genus-2 surface. This Riemann surface is known traditionally as the *Bolza surface* [31]. Accordingly, we shall refer to the regular $\{8, 8\}$ tessellation as the *Bolza lattice*. The Bolza surface is but one Riemann surface in an entire *moduli space* of distinct Riemann surfaces of genus 2 [32]. In general, there are $3g - 3$ complex degrees of freedom to vary the Riemann surface structure whenever $g \geq 2$ — this is the dimension of the moduli space — while the underlying topological class has no freedom. Of the points in the moduli space, the Bolza surface is the Riemann surface of genus 2 with the largest possible automorphism group, reflecting the high degree of symmetry in the original lattice and its edge identifications. (We use automorphisms of Riemann surfaces to generalize the notion of point-group symmetry to hyperbolic lattices in Sec. III C.)

Now, we define the hyperbolic Bloch factor $\chi(\gamma)$ in Eq. (13) by its action on the generators (21),

$$\chi(\gamma_j) = \chi(\gamma_j^{-1})^* = e^{ik_j}, \quad j = 1, \dots, 4, \quad (24)$$

writing the hyperbolic crystal momentum (12) as $\mathbf{k} = (k_1, k_2, k_3, k_4) \in \text{Jac}(\Sigma_2)$. Indeed, in this case, the underlying topology of the hyperbolic Brillouin zone $\text{Jac}(\Sigma_2)$ is a four-dimensional torus T^4 . Since we require χ to be a representation of Γ , we further define $\chi(\gamma_i \gamma_j) = \chi(\gamma_i) \chi(\gamma_j)$, for any $i, j = 1, \dots, 4$. Since Γ is finitely generated by the γ_j , this is sufficient to define $\chi(\gamma)$ for any $\gamma \in \Gamma$. Furthermore, Eq. (24) implies that χ satisfies the generator relation (23).

Combining the definition (24) of the hyperbolic Bloch factor with the automorphic Bloch condition (13) and the identifications (22), the four boundary conditions we impose when solving the hyperbolic Bloch problem (14) on the hyperbolic octagon \mathcal{D} become:

$$\psi(C_j) = e^{ik_j} \psi(C_{j+4}), \quad j = 1, \dots, 4. \quad (25)$$

A. The empty-lattice approximation

In ordinary band theory, the simplest problem that illustrates many salient features of generic bandstructures, including zone folding and symmetry-protected or accidental degeneracies, is the *empty-lattice approximation* [3]. In this approximation, the potential is taken to be constant, and thus necessarily periodic; without loss of generality, one can further choose $V = 0$. As we then have

$$H = H_0 = -\frac{\nabla^2}{2m}, \quad (26)$$

the problem thus reduces to finding the eigenvalues and eigenfunctions of the Euclidean Laplacian with the twisted periodic boundary conditions (8). One easily finds $E_{\mathbf{n}}(\mathbf{k}) = \frac{1}{2m}(\mathbf{k} + 2\pi\mathbf{n})^2$ and $\psi_{\mathbf{n}\mathbf{k}}(\mathbf{r}) \propto e^{i(\mathbf{k} + 2\pi\mathbf{n}) \cdot \mathbf{r}}$, with $\mathbf{k} \in [-\pi, \pi]^2 / \sim$ as the crystal momentum and $\mathbf{n} = (n_x, n_y) \in \mathbb{Z}^2$ as a discrete band index.

In the hyperbolic case, we wish to find the eigenvalues E and eigenfunctions ψ of the hyperbolic Laplacian $-\Delta$ on the hyperbolic octagon \mathcal{D} with the boundary conditions (25). At the origin of the hyperbolic Brillouin zone, $\mathbf{k} = 0$, those boundary conditions reduce to the condition that the solutions be strictly automorphic, $\psi(\gamma(z)) = \psi(z)$, the case usually considered in mathematics [34].

While exact analytical solutions for the eigenfunctions and eigenenergies are unavailable, this problem can be studied numerically. Motivated by questions in the theory of quantum chaos, approximate eigenenergies and eigenfunctions of the hyperbolic Laplacian on hyperbolic octagons with strictly automorphic boundary conditions were first obtained in Ref. [35] using the finite element method. Subsequent work studied this problem using the boundary element method [36], quantization via the Selberg trace formula [30], time-dependent methods [37], and an algorithm

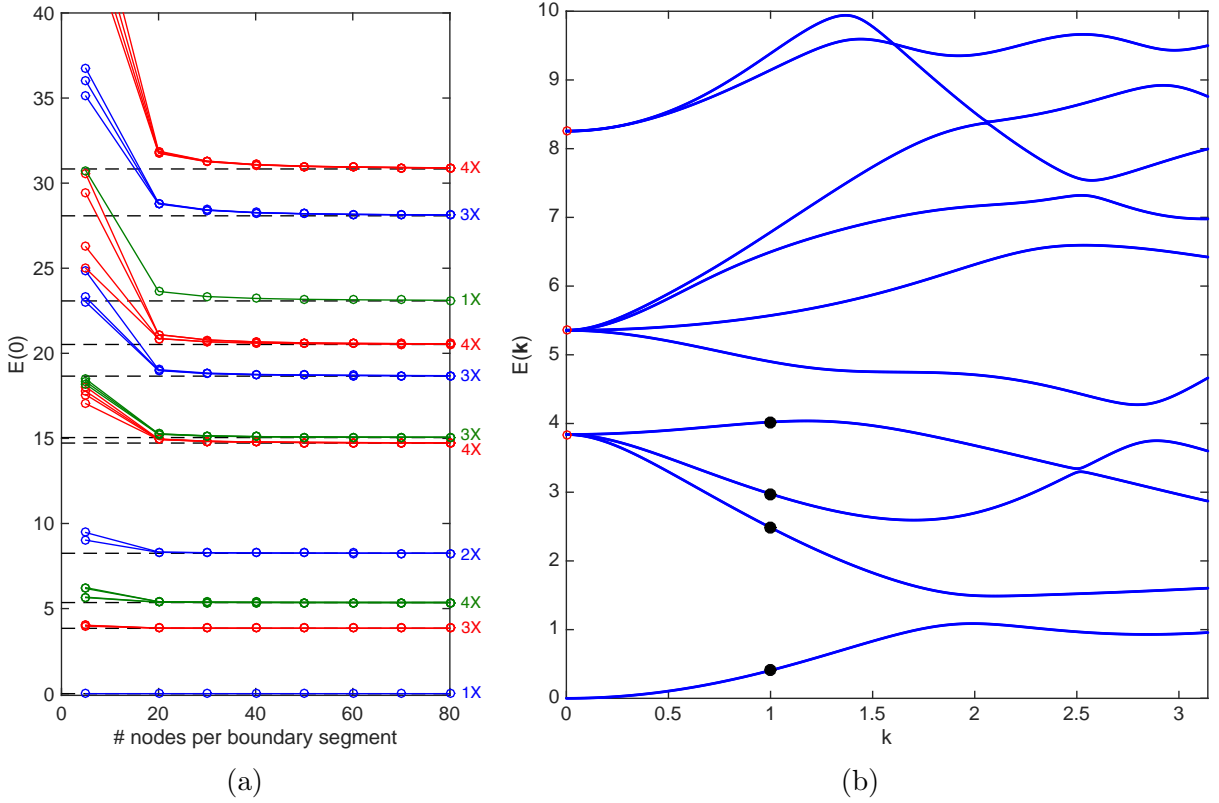


FIG. 2. Hyperbolic bandstructure of the Bolza lattice in the empty-lattice approximation. (a) $\mathbf{k} = 0$ eigenenergies computed using the finite element method (colored plots) vs eigenvalues of the Laplacian on the Bolza surface taken from Ref. [33] (dashed lines); only the lowest eleven distinct eigenvalues are shown (degeneracies from Ref. [33] shown on the right). The total number of mesh nodes grows approximately quadratically with the number of boundary nodes (see Fig. B.1). (b) Hyperbolic bandstructure plotted along a generic direction in the hyperbolic Brillouin zone: $\mathbf{k} = (k_1, k_2, k_3, k_4) = (0.8, 0.3, 1.2, 1.7)\mathbf{k}$. Red circles: eigenvalues of the Laplacian on the Bolza surface taken from Ref. [33]; black dots: eigenstates whose probabilities densities are plotted in Fig. 3(e-h).

based on the method of particular solutions [33]. In accordance with our previous expectations, the spectrum $\{E_n(0)\}$ of $-\Delta$ with strictly automorphic boundary conditions is indeed found to be real and discrete. For the Bolza surface of interest to us, the lowest eigenvalue is $E_0(0) = 0$, corresponding to a constant eigenfunction over \mathcal{D} , and the next three eigenvalues are given approximately by $E_1(0) \approx 3.839$, $E_2(0) \approx 5.354$, and $E_3(0) \approx 14.726$ [33].

Here, we study the general case $\mathbf{k} \neq 0$ for Σ_2 using the finite element method. We use a freely available software package, FreeFEM++ [38], which was used successfully to study the spectrum of the Bolza surface with strictly automorphic boundary conditions [39]. Our implementation of the twisted boundary conditions (25) is discussed in Appendix B. As a check on our calculations, we first compute the spectrum $\{E_n(0)\}$, i.e., with strictly automorphic boundary conditions [colored

plots in Fig. 2(a)]. With increased refinement of the finite element mesh, the $\mathbf{k} = 0$ spectrum gradually converges to previously obtained results [33]. In particular, the degeneracies found in Ref. [33, 39] are correctly reproduced with a sufficiently fine mesh. Such degeneracies are a consequence of the large symmetry group (automorphism group) of the Bolza surface [39], which can be thought of as the hyperbolic analog of a point group (see Sec. III C). We use a mesh with 70 nodes per boundary segment in all remaining plots, which achieves satisfactory accuracy at reasonable computational cost. Since the spectrum is unbounded, we only compute a small number of low-lying eigenvalues using standard numerical linear algebra techniques.

A well-known result in conventional band theory is that, ignoring spin degrees of freedom, degeneracies at high-symmetry points fully split as one moves away from such points along a generic direction in reciprocal space [3]. An example of a high-symmetry point is the origin $\mathbf{k} = 0$ of the Brillouin zone — equivalently, the group identity in $\text{Jac}(\Sigma_2)$. To ascertain whether this behavior holds in the hyperbolic case, we compute the hyperbolic bandstructure for $\mathbf{k} \neq 0$ along a generic direction in the hyperbolic Brillouin zone [Fig. 2(b)]. The lowest eigenvalue $E_0(0) = 0$ is nondegenerate at $\mathbf{k} = 0$ and thus does not split. As in the Euclidean case, the energy $E_0(\mathbf{k})$ of the lowest band increases with the magnitude of \mathbf{k} at small \mathbf{k} , in accordance with the intuitive expectation that (kinetic) energy increases with crystal momentum in the long-wavelength limit. The next three eigenvalues $E_1(0)$, $E_2(0)$, $E_3(0)$ are three-, four-, and two-fold degenerate, respectively [33, 39], but this degeneracy is completely lifted as \mathbf{k} moves away from zero, as in conventional band theory. We also observe linear crossings between some of the bands emanating from $E_2(0)$ and $E_3(0)$. According to the von Neumann-Wigner theorem [40], only codimension-3 level crossings are perturbatively stable in the absence of symmetries other than translational. Thus by contrast with 2D (or 3D) Euclidean lattices, we expect generically stable nodal-line crossings [41] in the hyperbolic bandstructures of $\{8, 8\}$ tessellations, and for general $\{4g, 4g\}$ tessellations, stable crossings forming $(2g - 3)$ -dimensional submanifolds of $\text{Jac}(\Sigma_g)$.

In algebraic geometry, the points of degeneracy are known as *ramification points* while the splitting-off of eigensheets is known as *branching*. From this point of view, the total energy manifold $E_n(\mathbf{k})$, for all n and for all \mathbf{k} , is a *branched cover* of $\text{Jac}(\Sigma_2)$, although not one of finite type, as there are countably- but not finitely-many levels n . Finite-type branched covers arising from eigenvalues of finite-rank linear operators, known as *spectral covers*, are studied frequently in algebraic geometry, especially in connection with gauge theories, integrable systems, and high-energy physics, e.g., Ref. [42].

Our finite element calculation also gives us access to the detailed spatial profile of the hyperbolic Bloch wavefunctions $\psi_{n\mathbf{k}}(z)$. Since these wavefunctions obey the automorphic Bloch condition (13) by construction, it is sufficient to plot them for z in the central hyperbolic octagon \mathcal{D} [Fig. 3]. At $\mathbf{k} = 0$, the wavefunctions are purely real. The ground state [Fig. 3(a)] is nodeless and perfectly uniform, while the excited states [Fig. 3(b-d)] acquire nodes. For $\mathbf{k} \neq 0$, the wavefunctions are in general complex, as in the Euclidean case. The probability densities for ground and excited states [Fig. 3(e-h)] are modulated by the \mathbf{k} vector with respect to their $\mathbf{k} = 0$ counterparts. (Note however

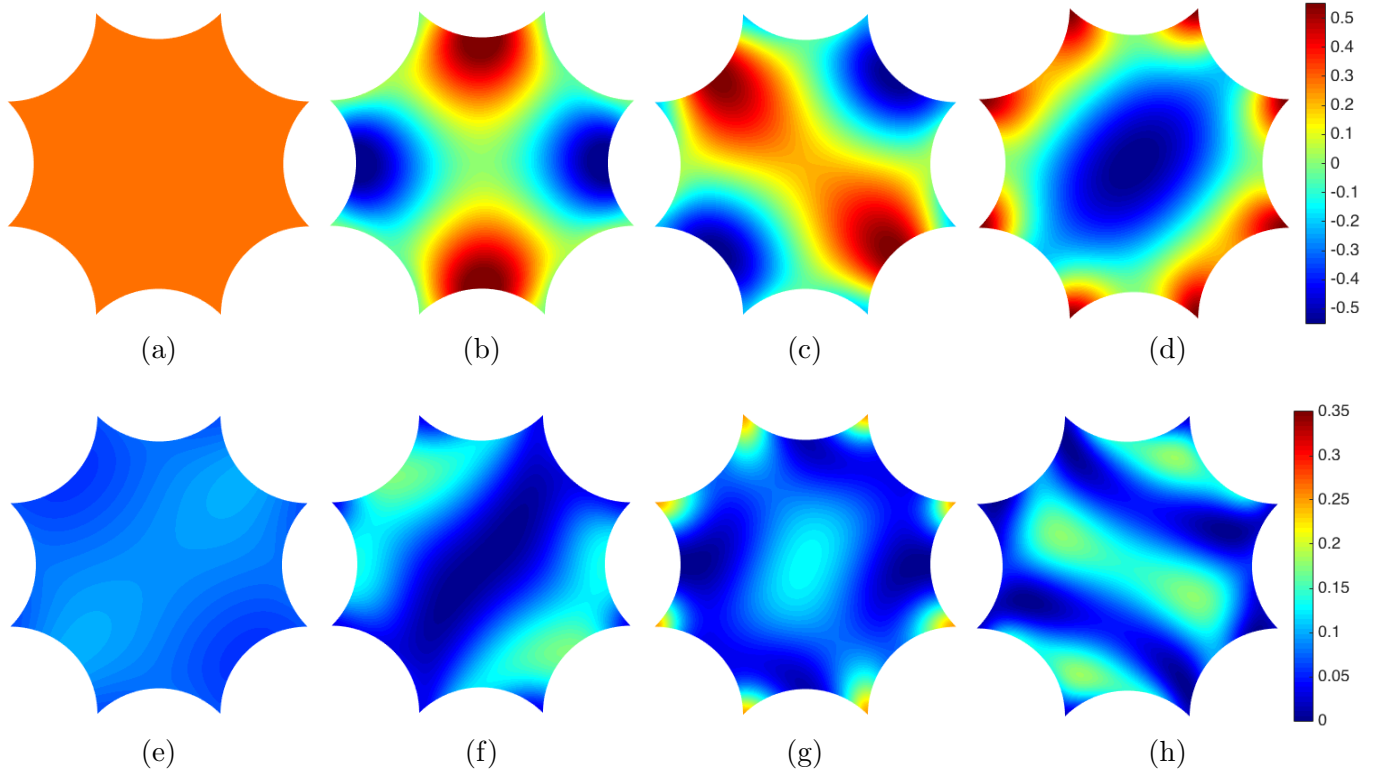


FIG. 3. Hyperbolic Bloch eigenstates in the empty-lattice approximation. Wavefunction $\psi_{\mathbf{k}}(z)$ for the (a) ground state and (b-d) degenerate first excited states at $\mathbf{k} = 0$; modulus squared $|\psi_{\mathbf{k}}(z)|^2$ for the (e) ground and (f-h) first three excited states corresponding to the black dots in Fig. 2(b), i.e., at $\mathbf{k} = (0.8, 0.3, 1.2, 1.7)$, in order of increasing eigenenergy.

that the three excited states in [Fig. 3(b-d)] are degenerate, and only represent one possible basis of the degenerate subspace, which is split at $\mathbf{k} \neq 0$; thus one cannot directly match [Fig. 3(b-d)] and [Fig. 3(f-h)].)

B. A particle in an automorphic potential

We now consider turning on a nonzero automorphic potential V . Such a potential can be constructed by summing over all Γ -translates of a localized potential $U(z)$,

$$V(z) = \sum_{\gamma \in \Gamma} U(\gamma(z)), \quad (27)$$

which is a kind of generalized theta series [14]. To ensure this series converges everywhere, we choose $U(z)$ with compact support in \mathcal{D} , for instance, a circular well of radius R and depth V_0 :

$$U(z) = \begin{cases} -V_0, & |z| < R, \\ 0, & |z| \geq R. \end{cases} \quad (28)$$

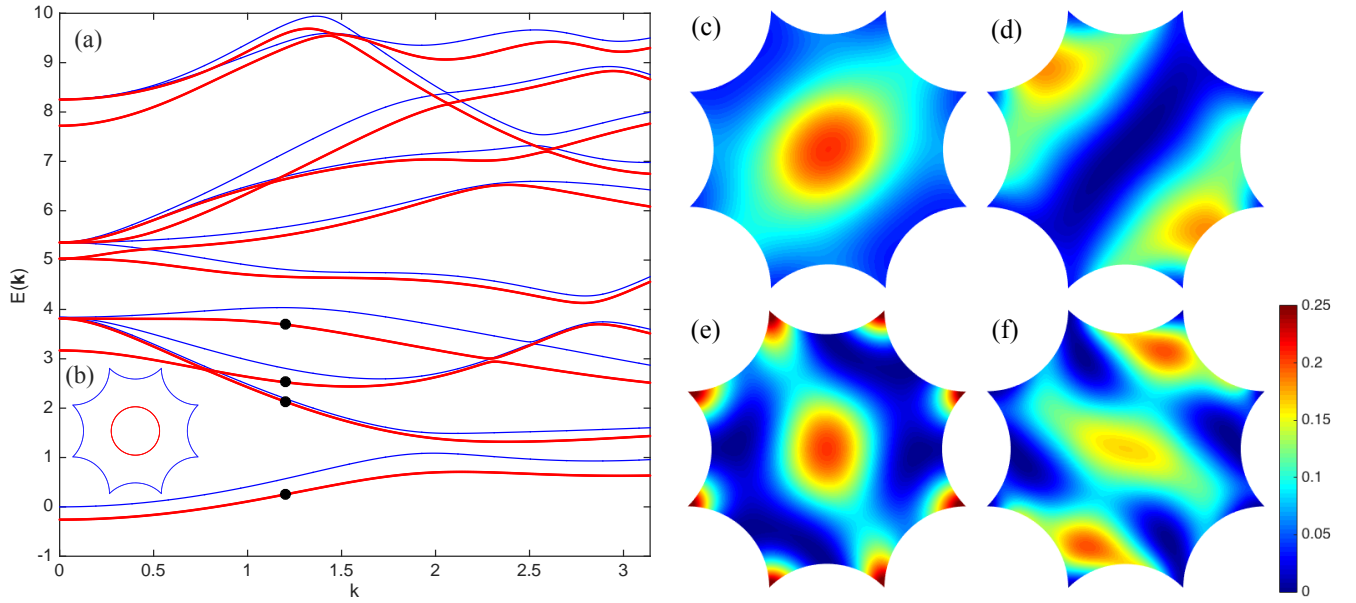


FIG. 4. Hyperbolic Bloch problem with nontrivial automorphic potential of the form (27). (a) Band-structure with (red) and without (blue) automorphic potential, along the same direction in the hyperbolic Brillouin zone as in Fig. 2; (b) circularly symmetric potential $U(z)$ in the octagonal unit cell, with $R = 0.3$ and $V_0 = 2$ [see Eq. (28)]; (c-f) modulus squared $|\psi_{\mathbf{k}}(z)|^2$ of the eigenstates corresponding to the black dots in (a), i.e., at $\mathbf{k} = (0.8, 0.3, 1.2, 1.7)\mathbf{k}$ with $k = 1.2$, in increasing order of eigenenergy.

As discussed in Sec. II, since the full Hamiltonian $H = -\Delta + V$ is invariant under Γ -translations, it is sufficient to solve the Schrödinger equation (14) with the automorphic Bloch boundary conditions (25) on \mathcal{D} .

In [Fig. 4(a)], we plot the hyperbolic bandstructure for the potential (27-28) with $R = 0.3$ and $V_0 = 2$, illustrated schematically in the inset [Fig. 4(b)]. Focusing first on the $\mathbf{k} = 0$ eigenenergies, we find that the ground-state energy is lowered from $E_0(0) = 0$ to a negative value, as expected for an attractive potential. We observe a (partial) lifting of the $\mathbf{k} = 0$ degeneracies: the 3-fold degeneracy of $E_1(0)$ is split as $2 \oplus 1$; the 4-fold degeneracy of $E_2(0)$, as $2 \oplus 2$; and the 2-fold degeneracy of $E_3(0)$ is lifted. For both the first and second excited spectral manifolds, we find the energy of one of the doublets is virtually unchanged from the original unperturbed eigenvalue. For the first excited manifold, this can be understood from the fact that for two of the three unperturbed eigenstates [Fig. 3(b-c)], most of the probability density is concentrated near the boundary segments, with very little near the center of the octagon. From the perspective of degenerate perturbation theory, the average of the potential (28) over the appropriate linear combinations would yield a small correction to the eigenenergies. By contrast, the third unperturbed eigenfunction [Fig. 3(d)] has modulus squared peaked near the center of the octagon, and also at its corners: it registers the potential more, and the correction to its eigenenergy is correspondingly greater.

In [Fig. 4(c-f)] we plot the modulus squared of the hyperbolic Bloch wavefunctions corresponding

to the (nondegenerate) levels indicated by black dots in [Fig. 4(a)]. For the lowest band [Fig. 4(c)], due to the attractive potential the probability density is much more concentrated near the center of the unit cell, as compared to the empty-lattice approximation [e.g. [Fig. 3(e)], although the value of \mathbf{k} is not exactly the same]. The eigenfunctions for the next three bands [Fig. 4(d-f)] are also distorted with respect to their empty-lattice counterparts [Fig. 3(f-h)]. The observation that the probability density in [Fig. 4(e)] is peaked near the center and at the corners of the octagonal unit cell, combined with the fact that at $\mathbf{k} = 0$ this same hyperbolic Bloch state belongs to the singlet in the splitting $3 \rightarrow 2 \oplus 1$ discussed above for the $E_1(0)$ spectral manifold, confirms our earlier speculation concerning the qualitative reason for this splitting.

C. Point-group symmetries and automorphisms of Riemann surfaces

We have so far only discussed the hyperbolic analog of lattice translations, namely, elements of a co-compact, strictly hyperbolic Fuchsian group $\Gamma \subset PSL(2, \mathbb{R})$. Like Euclidean translations, these elements act on the hyperbolic plane without fixed points, and are essentially 2D Lorentz boosts [43]. Also akin to Euclidean lattices, hyperbolic lattices admit the analog of point-group symmetries, which are discrete symmetries that leave at least one point of the lattice fixed. A complete hyperbolic band theory must also include a discussion of these, with particular attention paid to how such point-group symmetries manifest in \mathbf{k} -space.

For a 2D Euclidean lattice, the point group G is a finite subgroup of the orthogonal group $O(2)$, which includes $SO(2)$ rotations but also orientation-reversing transformations, that is, reflections. Point-group symmetries imply that if $\psi_{\mathbf{k}}(\mathbf{r})$ is a Bloch eigenstate for such a lattice with energy $E(\mathbf{k})$, the transformed state $\psi_{\mathbf{k}}^h(\mathbf{r}) \equiv \psi_{\mathbf{k}}(h\mathbf{r})$, with $h \in G$, is also an eigenstate with the same energy. By elementary properties of Fourier transforms, this transformed state is in fact a Bloch state with wavevector $\mathbf{k}^h \equiv h\mathbf{k}$, which implies that the bandstructure must obey $E(h\mathbf{k}) = E(\mathbf{k})$.

In the absence of an abelian translation group, Fourier transforms cannot be directly used to generalize these ideas to hyperbolic lattices. Furthermore, since for a $\{4g, 4g\}$ hyperbolic lattice \mathbf{k} -space is in fact $4g$ -dimensional, the very question of how non-translational discrete symmetries in 2D hyperbolic space act in a higher-dimensional \mathbf{k} -space is a deep conceptual one. That said, given that the Abel-Jacobi map provides an algebraic replacement for the Fourier transform, this duality provides a potentially lucrative route for exploring the effect of point-group symmetries. As the group acts on Σ_g , it acts on the symmetric product of Σ_g with itself and, hence, on $\text{Jac}(\Sigma_g)$ via Abel-Jacobi. As the action moves the points p_1, \dots, p_g in Σ_g , it moves the end points of the paths of integration in the definition of the map a from Sec. IID, which is the induced action on $\text{Jac}(\Sigma_g)$. We recall that there is a high-symmetry region within the Jacobian — in this region, the action may have more fixed points. We aim to utilize this point of view in further work.

For the specific case of the Bolza curve, we are able to examine the point-group action directly. Via concrete calculations for the Bolza lattice, we argue in Appendix C that the proper generalization of point group for $\{4g, 4g\}$ hyperbolic lattices is the finite group $G \cong \text{Aut}(\Sigma_g)$ of

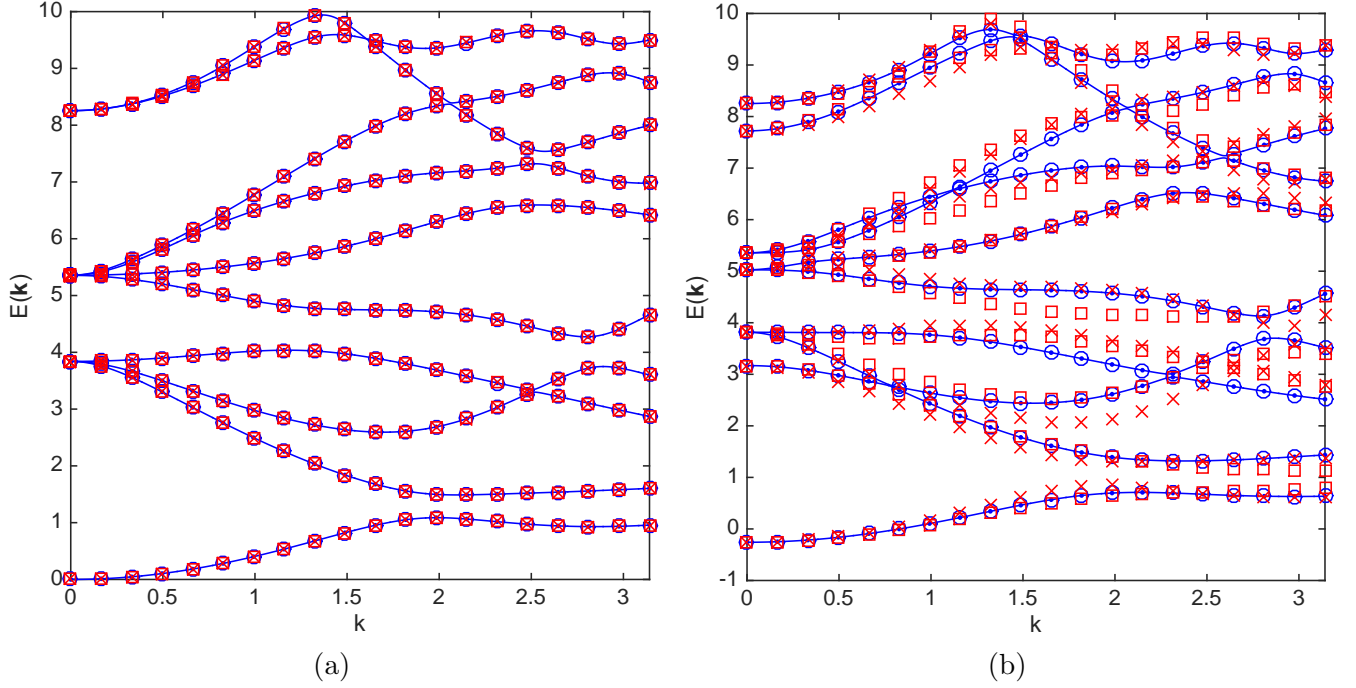


FIG. 5. Point-group symmetries in hyperbolic \mathbf{k} -space, (a) in the empty-lattice approximation and (b) with the automorphic potential of Fig. 4. Blue lines: hyperbolic bandstructure $E_n(\mathbf{k})$ along the direction of Figs. 2 and 4, blue dots: $E_n(\mathbf{k}^R)$, blue circles: $E_n(\mathbf{k}^S)$, red crosses: $E_n(\mathbf{k}^T)$, red squares: $E_n(\mathbf{k}^U)$.

automorphisms (i.e., self-maps) of the genus- g Riemann surface [21] associated with the “compactified” $4g$ -gonal unit cell. For the Bolza surface, it is a nonabelian group of order 96 generated by four Möbius transformations [39]: an eightfold rotation (R) around the center of the octagon and a threefold rotation-like operation (U), both orientation-preserving, and two reflection-like operations (S and T), both orientation-reversing. Furthermore, as in the Euclidean case, we find this “hyperbolic point group” acts linearly on hyperbolic \mathbf{k} -space:

$$\mathbf{k}^h = M(h)\mathbf{k}, \quad h \in G, \quad (29)$$

where the 4×4 matrices $M(h)$, $h \in G$, form an $SL(4, \mathbb{Z})$ representation of G . Explicit representation matrices for the generators $h = R, S, T, U$, from which the representation matrix of any element of G can be constructed by matrix multiplication, are given in Eq. (C.55) of Appendix C. For a $\{4g, 4g\}$ hyperbolic lattice, we conjecture that Eq. (29) remains valid, with M a representation of G valued in $SL(2g, \mathbb{Z})$. By contrast with the Euclidean case however, the matrices $M(h)$ are in general not orthogonal, and thus do not simply correspond to the action of a Euclidean point group in $2g$ dimensions.

In [Fig. 5(a)], we verify numerically that the hyperbolic bandstructure in the empty-lattice approximation is invariant under the full hyperbolic point group G of the Bolza lattice, meaning that $E_n(\mathbf{k}^h) = E_n(\mathbf{k})$ for all $h \in G$. We choose \mathbf{k} along the generic direction already considered in

[Fig. 2] and plot both $E_n(\mathbf{k})$ (blue lines) and $E_n(\mathbf{k}^h)$ (colored symbols), where \mathbf{k}^h is the direction related to \mathbf{k} by point-group symmetry h . We verify that the bandstructure is left unchanged under the action of all four generators $h = R, S, T, U$ of G , thus establishing invariance under the full point group.

[Fig. 5(a)] is to be contrasted with [Fig. 5(b)], which illustrates that the automorphic potential chosen in Eq. (27-28) breaks at least some of the hyperbolic point-group symmetries of the Bolza lattice. The R operation is a $\pi/4$ rotation about the origin, and the S operation is a reflection across the x axis followed by a $\pi/4$ rotation. Though formally defined as Möbius transformations, they reduce to simple Euclidean isometries that are obvious symmetries of the circular potential well (28). As a result, the bandstructure is left unchanged under $\mathbf{k} \rightarrow \mathbf{k}^h$ with $h = R, S$. By contrast, the T and U operations are genuine non-Euclidean isometries involving boosts (see Appendix C) that do not leave the potential (28) invariant. Correspondingly, the bandstructure does not exhibit invariance under $\mathbf{k} \rightarrow \mathbf{k}^h$ with $h = T, U$.

D. The tight-binding limit and Wannier functions

In conventional band theory, the tight-binding method is a commonly-used approximation scheme to analyze the Schrödinger equation in the limit of deep periodic potentials [3]. While inexact, it provides a conceptually important, and often sufficiently accurate, framework to study the Bloch problem in this limit. The tight-binding method starts from the discrete spectrum and localized eigenstates of isolated potential wells, and builds on the idea that propagation throughout the crystal proceeds via weak quantum tunneling between those localized states. Our hyperbolic band theory described so far is based on the full Schrödinger equation, and applies to arbitrary $\{4g, 4g\}$ automorphic potentials, including deep ones. However, to further develop our generalization of band theory and in light of the experiments of Ref. [8], which are most simply modelled using the tight-binding method, it is natural to ask whether an explicit tight-binding formulation of hyperbolic band theory can be devised. We now show this is indeed possible.

Consider first the quantum mechanics of an isolated, deep potential well $U(z)$ with compact support in \mathcal{D} , e.g., Eq. (28) with V_0 large. As with other potentials (e.g., Ref. [44]), we expect a number of bound states with discrete eigenenergies ϵ_n and localized wavefunctions $\phi_n(z)$, orthonormal with respect to the Poincaré metric, and satisfying an atomic-like Schrödinger equation:

$$(-\Delta + U(z))\phi_n(z) = \epsilon_n\phi_n(z), \quad z \in \mathbb{H}. \quad (30)$$

If the ϕ_n are sufficiently localized, they and their Γ -translates $\phi_n(\gamma(z))$, $\gamma \in \Gamma$, should be good approximations to the true wavefunctions of the full hyperbolic lattice with automorphic potential (27). To construct an approximate eigenstate that obeys the automorphic Bloch condition (13) with hyperbolic crystal momentum \mathbf{k} , we take an appropriate linear combination of those localized

wavefunctions,

$$\psi_{\mathbf{k}}(z) \approx \sum_{\gamma \in \Gamma} \sum_n b_{n\mathbf{k}} \chi_{\mathbf{k}}^*(\gamma) \phi_n(\gamma(z)), \quad (31)$$

where n ranges over the discrete levels of the atomic problem (30), $b_{n\mathbf{k}}$ is an expansion coefficient, and we explicitly indicated by a subscript the dependence of the Bloch phase factor (24) on \mathbf{k} . Substituting this approximate expansion into the full Schrödinger equation (14), multiplying from the left on both sides by $\phi_m^*(z)$, and integrating over the entire Poincaré disk, we obtain a hyperbolic analog of the standard tight-binding equations [3]:

$$\sum_n (\epsilon_m s_{mn}(\mathbf{k}) - u_{mn} - t_{mn}(\mathbf{k})) b_{n\mathbf{k}} \approx E(\mathbf{k}) \sum_n s_{mn}(\mathbf{k}) b_{n\mathbf{k}}, \quad (32)$$

a generalized matrix eigenvalue problem whose eigenvalues are approximate hyperbolic band energies $\{E_n(\mathbf{k})\}$ and whose eigenvectors are the expansion coefficients $b_{n\mathbf{k}}$. We define the overlap matrix $s_{mn}(\mathbf{k})$, the on-site potential matrix u_{mn} , and the hopping matrix $t_{mn}(\mathbf{k})$ as

$$s_{mn}(\mathbf{k}) = \delta_{mn} + \sum_{\gamma \neq e} \chi_{\mathbf{k}}^*(\gamma) \int_{\mathbb{H}} d^2 z \sqrt{g} \phi_m^*(z) \phi_n(\gamma(z)), \quad (33)$$

$$u_{mn} = - \int_{\mathbb{H}} d^2 z \sqrt{g} \phi_m^*(z) \Delta V(z) \phi_n(z), \quad (34)$$

$$t_{mn}(\mathbf{k}) = - \sum_{\gamma \neq e} \chi_{\mathbf{k}}^*(\gamma) \int_{\mathbb{H}} d^2 z \sqrt{g} \phi_m^*(z) \Delta V(z) \phi_n(\gamma(z)), \quad (35)$$

and $\Delta V = \sum_{\gamma \neq e} U(\gamma(z))$ is the sum (27) of Γ -translates of $U(z)$, excluding the reference cell \mathcal{D} .

Another key notion of conventional band theory, conceptually related to the tight-binding approximation, is that of Wannier functions [3]. In the Euclidean context, these are defined as the exact Fourier coefficients $f_n(\mathbf{R}, \mathbf{r})$ of a true Bloch eigenstate $\psi_{n\mathbf{k}}(\mathbf{r})$, expanded for each \mathbf{r} as a Fourier series in \mathbf{k} , with $\mathbf{R} \in \mathbb{Z}^2$ the sites of the real-space lattice. Since $\psi_{n\mathbf{k}}(\mathbf{r})$ satisfies the Bloch condition, Wannier functions are invariant under simultaneous translations of \mathbf{r} and \mathbf{R} by a given lattice vector $\mathbf{m} \in \mathbb{Z}^2$, and are thus necessarily of the form $f_n(\mathbf{r} - \mathbf{R})$. They can be interpreted as atomic-like wavefunctions associated with site \mathbf{R} , analogous to the atomic orbitals $\phi_n(\mathbf{r} - \mathbf{R})$ of the tight-binding approximation—the Euclidean analogs of our $\phi_n(\gamma(z))$. To construct a hyperbolic analog of Wannier functions, owing to the periodicity of the Jacobian one can likewise expand a hyperbolic Bloch eigenstate $\psi_{n\mathbf{k}}(z)$ as a Fourier series in \mathbf{k} , but now the Fourier components $f_n(\mathbf{R}, z)$ will be defined over a 4-dimensional Euclidean lattice $\mathbf{R} \in \mathbb{Z}^4$:

$$f_n(\mathbf{R}, z) = \int_{\text{Jac}(\Sigma_2)} \frac{d^4 k}{(2\pi)^4} e^{-i\mathbf{k} \cdot \mathbf{R}} \psi_{n\mathbf{k}}(z), \quad (36)$$

with obvious generalization to genus $g \geq 2$. We show in Appendix D that, like Euclidean Wannier functions, these hyperbolic Wannier functions are orthonormal. However, since z and \mathbf{R} live

in spaces of different dimensions, they cannot obey the same invariance property as Euclidean Wannier functions, but rather an automorphic analog thereof (see Appendix D):

$$f_n(\mathbf{R} + \mathbf{m}, \gamma_{\mathbf{m}}(z)) = f_n(\mathbf{R}, z), \quad (37)$$

where $\mathbf{m} = (m_1, m_2, m_3, m_4) \in \mathbb{Z}^4$ and $\gamma_{\mathbf{m}}$ is any Γ -translation such that $\chi_{\mathbf{k}}(\gamma_{\mathbf{m}}) = e^{i\mathbf{k} \cdot \mathbf{m}}$, e.g., $\gamma_{\mathbf{m}} = \gamma_1^{m_1} \gamma_2^{m_2} \gamma_3^{m_3} \gamma_4^{m_4}$.

IV. CONCLUSION

In summary, we have presented a generalization of band theory applicable to a large class of non-Euclidean lattices, $\{4g, 4g\}$ hyperbolic tessellations, borrowing several concepts from Riemann surface theory and algebraic geometry. Despite the absence of an abelian translation group, hyperbolic Bloch eigenstates can be constructed, based on the following key observation: for both Euclidean and hyperbolic lattices, the set of crystal momenta can be identified with the set of $2g$ Aharonov-Bohm phases threading the noncontractible cycles of the compact Riemann surface of genus g that results from identifying pairwise the sides of the unit cell under a suitable group, whether abelian or not, of generalized lattice translations. For hyperbolic lattices, one has $g \geq 2$ and this generalized translation group, the Fuchsian group Γ , is necessarily nonabelian. The higher-genus/hyperbolic crystal momentum — which reduces to ordinary crystal momentum in the Euclidean, genus-1 case — lives in a $2g$ -dimensional torus identified with a classical object in algebraic geometry: the Jacobian of the Riemann surface. The Abel-Jacobi map, another important result in algebraic geometry, maps any point inside the spatial unit cell to a point in the Jacobian and thus provides a hyperbolic analog of the Fourier/particle-wave duality between real space and momentum space. Hyperbolic Bloch eigenstates become automorphic functions with factor of automorphy given by a generalized Bloch phase factor, and the hyperbolic bandstructure forms a branched cover of the Jacobian. Point-group symmetries are identified with the finite group of automorphisms of the Riemann surface; they act in a nontrivial way on the Jacobian, and become symmetries of the hyperbolic bandstructure. Hyperbolic analogs of the tight-binding approximation and Wannier functions also follow naturally from these constructions.

Our work opens up several future avenues of research. While we have shown how to construct a continuous family of Bloch eigenstates for a large class of Hamiltonians with the symmetry of a hyperbolic tessellation, we have *not* provided a hyperbolic equivalent of Bloch's theorem—that is, a statement that *all* eigenstates of the Hamiltonian are hyperbolic Bloch eigenstates. What precise fraction of the full spectrum is captured by the hyperbolic Bloch family of eigenstates, and the nature of those eigenstates that may not be of hyperbolic Bloch form, are thus important questions for future research. One obvious line of attack is to attempt to match our predictions with those obtained from numerical diagonalization on $\{4g, 4g\}$ lattices, keeping in mind possible subtle issues related to the implementation of automorphic boundary conditions in finite lattices, especially given the different relative importance of bulk versus boundary in Euclidean versus

hyperbolic geometries. It may also be possible to approach those spectral questions using number-theoretic tools such as the Selberg trace formula and associated zeta function [23, 45]. Even within the Bloch condition, the role of factors of automorphy of nonzero weight is an intriguing question in the hyperbolic setting.

In further pursuing the connections to algebraic geometry and number theory, we note that higher-dimensional versions of our construction may be produced now for K3 surfaces and Calabi-Yau manifolds (e.g., [46]), which generalize elliptic curves, and for Shimura varieties (e.g., [47]), which generalize modular curves. Working over Calabi-Yau manifolds is especially tantalizing as a potential pathway for novel connections between high-energy physics and condensed matter, which may offer new tools to the latter from string theory and mirror symmetry (e.g., [48]). In three spatial dimensions specifically, we also anticipate connections with the work of Thurston [49], whereby hyperbolic bandstructures may arise in connection with three-dimensional hyperbolic tessellations, their (Kleinian) groups of discrete translations, and the geometry and topology of compact three-manifolds produced by the quotienting of three-dimensional hyperbolic space by Kleinian translations. Finally, on the experimental side, we advocate the fabrication and characterization of $\{4g, 4g\}$ lattices using circuit QED [8], photonic [13], or other metamaterial platforms.

Our construction carries with it a realization that our topological understanding of condensed matter is a small corner of a theory that is perhaps, by and large, algebro-geometric in nature. Indeed, our construction anticipates the emergence of algebro-geometric invariants alongside topological ones, such as Donaldson-Thomas invariants [50] of higher-dimensional complex varieties.

ACKNOWLEDGMENTS

The authors wish to thank M. Protter for assisting with some of the derivations in Appendices B and C, and G. Shankar for assisting with some of the derivations in Appendix A.

The authors also acknowledge helpful conversations with M. Berg, V. Bouchard, R. Boyack, T. Creutzig, C. Doran, D. Freed, T. Gannon, C. Mahadeo, R. Mazzeo, A. Neitzke, A. Stevens, J. Szmigielski, and K. Tanaka. While working on the research reported in this manuscript, JM was supported by NSERC Discovery Grants #RGPIN-2014-4608, #RGPIN-2020-06999, and #RGPAS-2020-00064; the Canada Research Chair (CRC) Program; CIFAR; the Government of Alberta’s Major Innovation Fund (MIF); and the University of Alberta. SR was supported by NSERC Discovery Grant #RGPIN-2017-04520; the Canada Foundation for Innovation John R. Evans Leaders Fund; the GEAR Network (National Science Foundation grants DMS 1107452, 1107263, 1107367 *RNMS: Geometric Structures and Representation Varieties*); the School of Mathematics and Physics at the University of Queensland (through the Ethel Raybould Fellowship program); and the University of Saskatchewan. Both JM and SR were supported by the Tri-Agency New Frontiers in Research Fund (NFRF, Exploration Stream) and the Pacific Institute for the Mathematical Sciences (PIMS) Collaborative Research Group program.

Appendix A: Fundamental group of the Bolza surface

The Bolza surface Σ_2 is a Riemann surface of genus 2 [31] obtained by identifying the opposite sides of the hyperbolic octagon in Fig. 1(c). Under this identification, the eight vertices p_1, \dots, p_8 of the octagon are mapped to a single point p_0 which we can take as the base point for loops [19]. Under the identification, each of the eight geodesic boundary segments C_1, \dots, C_8 starts and ends at p_0 and is thus a closed loop; thus the C_j , $j = 1, \dots, 8$ are elements of the fundamental group $\pi_1(\Sigma_2, p_0)$ based at p_0 . Consider a closed path C that starts at $p_1 \sim p_0$ and goes around the boundary of the octagon counterclockwise. Denoting by C_1, \dots, C_8 the oriented paths with orientations indicated by the arrows in Fig. 1(c), and by $C_1^{-1}, \dots, C_8^{-1}$ the same paths traversed in reverse, C is given by

$$C = C_1 C_2^{-1} C_3 C_4^{-1} C_5^{-1} C_6 C_7^{-1} C_8. \quad (\text{A.1})$$

Now, C can be continuously deformed to a point inside the octagon, thus it is homotopic to the trivial path: $C = 1$. This remains true after identification. After identification, however, C_j and C_{j+4} , $j = 1, \dots, 4$ are identified in an orientation-preserving manner. Therefore, the unique relation satisfied by the distinct generators C_1, C_2, C_3, C_4 of $\pi(\Sigma_2, p_0)$ is:

$$C_1 C_2^{-1} C_3 C_4^{-1} C_1^{-1} C_2 C_3^{-1} C_4 = 1. \quad (\text{A.2})$$

Since fundamental groups with different base points are isomorphic, we can simply write:

$$\pi_1(\Sigma_2) = \{C_1, C_2, C_3, C_4 : C_1 C_2^{-1} C_3 C_4^{-1} C_1^{-1} C_2 C_3^{-1} C_4 = 1\}. \quad (\text{A.3})$$

Isomorphic groups may have different, but equivalent, presentations. For example, one can give a different presentation for (A.3) as follows [30]. Define new generators as $a_1 = C_3$, $b_1 = C_4^{-1}$, $a_2 = C_1 C_2^{-1}$, and $b_2 = C_3 C_4^{-1} C_1^{-1}$. Then using (A.2), one finds that the relation satisfied by these new generators is that of Eq. (10) with $g = 2$. Correspondingly, the original generators can be obtained from the new ones by $C_1 = b_2^{-1} a_1 b_1$, $C_2 = a_2^{-1} b_2^{-1} a_1 b_1$, $C_3 = a_1$, and $C_4 = b_1^{-1}$. Since products of homotopy classes correspond to composition of loops, different choices of generators correspond to different choices of closed loops on the Riemann surface. In Sec. III, our choice of representation $\chi : \pi_1(\Sigma_2) \rightarrow U(1)$ in Eq. (24) associates k_1, k_2, k_3, k_4 with the Aharonov-Bohm acquired upon traversing C_1, C_2, C_3, C_4 , but the choice (11) with a_1, b_1, a_2, b_2 defined above is equally valid. It can simply be thought of as the choice of a different basis for the hyperbolic reciprocal lattice, i.e., the $2g$ -dimensional lattice Λ such that the quotient $\mathbb{R}^{2g} \cong \mathbb{C}^g$ by it gives $\text{Jac}(\Sigma_g) \cong T^{2g}$.

Appendix B: Twisted automorphic boundary conditions in the finite element method

The FreeFEM++ package [38] allows for Dirichlet, Neumann, or strictly periodic/automorphic boundary conditions, but not directly for the twisted automorphic boundary conditions required

for nonzero \mathbf{k} [Eq. (25)]. To remedy this problem, we follow the approach of Refs. [51–53], in which the stiffness and overlap matrices of the weak (variational) formulation of the hyperbolic Schrödinger equation (14) are first computed using FreeFEM++ with unconstrained boundary conditions, and the number of physical degrees of freedom is subsequently reduced using simple matrix operations before proceeding to numerical diagonalization. The generalized Bloch phases (25) are easily introduced at this second stage, as we now explain.

Consider two functions ϕ, ψ obeying the twisted automorphic condition (13). The weak form of the partial differential equation (14) is obtained by multiplying this equation by ϕ^* and integrating over the domain \mathcal{D} ,

$$\int_{\mathcal{D}} d^2r \sqrt{g} (-\phi^* \Delta \psi + \phi^* V \psi) = E \int_{\mathcal{D}} d^2r \sqrt{g} \phi^* \psi, \quad (\text{B.1})$$

where $\sqrt{g} = 4/(1 - |z|^2)^2$ is the square root of the determinant of the Poincaré metric tensor $g_{\mu\nu} = 4\delta_{\mu\nu}/(1 - |z|^2)^2$ in Eq. (2), and $d^2r = dx dy$ is the usual Euclidean integration measure. Using Green’s theorem and the condition (13), one can show that Eq. (B.1) becomes [23]

$$\int_{\mathcal{D}} d^2r \sqrt{g} (g^{\mu\nu} \partial_{\mu} \phi^* \partial_{\nu} \psi + \phi^* V \psi) = E \int_{\mathcal{D}} d^2r \sqrt{g} \phi^* \psi. \quad (\text{B.2})$$

Using the inverse metric tensor $g^{\mu\nu} = \frac{1}{4} \delta^{\mu\nu} (1 - |z|^2)^2$, we obtain

$$\int_{\mathcal{D}} d^2r \left(\partial_x \phi^* \partial_x \psi + \partial_y \phi^* \partial_y \psi + \frac{4\phi^* V \psi}{(1 - |z|^2)^2} \right) = E \int_{\mathcal{D}} d^2r \frac{4\phi^* \psi}{(1 - |z|^2)^2}. \quad (\text{B.3})$$

In the finite element method, one triangulates the region \mathcal{D} (e.g., Fig. B.1) and expands the solution ψ on a basis of functions u_i , $i = 1, \dots, M$ with compact support on each finite element (i.e., triangle) in the triangulation. While M is formally infinite, in practice, we truncate $\{u_i\}$ to the set of linear Lagrangian shape functions (P1 elements in the notation of Ref. [38]). M then equals the finite number of vertices in the triangulation, and the piecewise-linear basis function u_i equals one on vertex i and vanishes on all other vertices. While simple, the choice of P1 elements allows us to achieve satisfactory accuracy with a sufficiently fine triangulation. Expanding $\psi = \sum_{j=1}^M \psi_j u_j$ and taking $\phi = u_i$, Eq. (B.3) becomes

$$\sum_{j=1}^M A_{ij} \psi_j = E \sum_{j=1}^M B_{ij} \psi_j, \quad i = 1, \dots, M, \quad (\text{B.4})$$

where the $M \times M$ Hermitian matrices A (stiffness matrix) and B (overlap matrix) are

$$A_{ij} = \int_{\mathcal{D}} d^2r \left(\partial_x u_i^* \partial_x u_j + \partial_y u_i^* \partial_y u_j + \frac{4u_i^* V u_j}{(1 - |z|^2)^2} \right), \quad B_{ij} = \int_{\mathcal{D}} d^2r \frac{4u_i^* u_j}{(1 - |z|^2)^2}. \quad (\text{B.5})$$

The solution of the Schrödinger equation (14) in continuous space is thus approximated by the solution of a finite-dimensional generalized eigenvalue problem, Eq. (B.4).

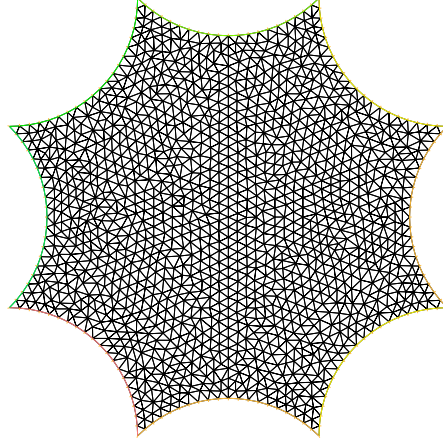


FIG. B.1. A finite element triangulation of the hyperbolic octagon \mathcal{D} with 20 nodes per boundary segment.

We now explain how to impose the boundary conditions (25). Since i, j are vertex indices, the solution vector $\boldsymbol{\psi} = (\psi_1, \dots, \psi_M)$ can be written in block form as

$$\boldsymbol{\psi} = (\psi_{p_1}, \dots, \psi_{p_8}; \boldsymbol{\psi}_{C_1}, \dots, \boldsymbol{\psi}_{C_8}; \boldsymbol{\psi}_{\text{bulk}}), \quad (\text{B.6})$$

in the notation of Fig. 1(c), where p_1, \dots, p_8 denote vertices at the eight corners of the hyperbolic octagon; $\boldsymbol{\psi}_{C_j}$, $j = 1, \dots, 8$, is a vector containing the solution on the set of vertices belonging to the boundary segment C_j of the octagon, excluding corners; and $\boldsymbol{\psi}_{\text{bulk}}$ is a vector containing the solution on the interior vertices. The boundary conditions, which identify boundary segments (including corners) pairwise, imply that only $N < M$ degrees of freedom are in fact independent. There thus exists an $M \times N$ matrix U such that $\boldsymbol{\psi} = U\tilde{\boldsymbol{\psi}}$, where $\tilde{\boldsymbol{\psi}}$ is an N -dimensional vector containing only the independent degrees of freedom. Substituting this equation inside the M -dimensional generalized eigenvalue problem $A\boldsymbol{\psi} = EB\boldsymbol{\psi}$ in (B.4), and left-multiplying by U^\dagger , we obtain the reduced, N -dimensional generalized eigenvalue problem:

$$\tilde{A}\tilde{\boldsymbol{\psi}} = E\tilde{B}\tilde{\boldsymbol{\psi}}, \quad (\text{B.7})$$

where

$$\tilde{A} = U^\dagger A U, \quad \tilde{B} = U^\dagger B U, \quad (\text{B.8})$$

are again Hermitian.

The $M \times N$ matrix U is constructed as follows. First, the bulk vertices are unaffected by the boundary conditions, thus $\boldsymbol{\psi}_{\text{bulk}}$ appears in full in $\tilde{\boldsymbol{\psi}}$. Next, out of the eight boundary vectors $\boldsymbol{\psi}_{C_1}, \dots, \boldsymbol{\psi}_{C_8}$, only four are linearly independent due to the boundary conditions. Using Eq. (25),

we can thus express all eight boundary vectors in terms of $\psi_{C_5}, \dots, \psi_{C_8}$:

$$\begin{pmatrix} \psi_{C_1} \\ \psi_{C_2} \\ \psi_{C_3} \\ \psi_{C_4} \\ \psi_{C_5} \\ \psi_{C_6} \\ \psi_{C_7} \\ \psi_{C_8} \end{pmatrix} = \begin{pmatrix} e^{ik_1} & & & & & & & \\ & e^{ik_2} & & & & & & \\ & & e^{ik_3} & & & & & \\ & & & e^{ik_4} & & & & \\ & 1 & & & & & & \\ & & 1 & & & & & \\ & & & 1 & & & & \\ & & & & 1 & & & \end{pmatrix} \begin{pmatrix} \psi_{C_5} \\ \psi_{C_6} \\ \psi_{C_7} \\ \psi_{C_8} \end{pmatrix}, \quad (\text{B.9})$$

making also sure that the components of the respective vectors are ordered so as to preserve orientation under pairwise identification [see Fig. 1(c)]. Finally, all eight corner vertices p_1, \dots, p_8 collapse under this identification to a single point, which can be chosen as p_5 . Using the action of the Fuchsian group generators depicted in Fig. 1(c), we can express the remaining vertices as:

$$\begin{aligned} p_1 &= \gamma_1 \gamma_4 \gamma_3^{-1} \gamma_2(p_5), & p_2 &= \gamma_2(p_5), & p_3 &= \gamma_4 \gamma_1(p_5), & p_4 &= \gamma_4 \gamma_3^{-1} \gamma_2(p_5), \\ p_6 &= \gamma_3^{-1} \gamma_4 \gamma_1(p_5), & p_7 &= \gamma_3^{-1} \gamma_2(p_5), & p_8 &= \gamma_1(p_5). \end{aligned} \quad (\text{B.10})$$

Note that this choice of representation is not unique, but different representations can be shown to be equivalent using the relation (23). Using the generalized Bloch factor (24), we can thus write

$$\begin{pmatrix} \psi_{p_1} \\ \psi_{p_2} \\ \psi_{p_3} \\ \psi_{p_4} \\ \psi_{p_5} \\ \psi_{p_6} \\ \psi_{p_7} \\ \psi_{p_8} \end{pmatrix} = \begin{pmatrix} e^{i(k_1+k_2-k_3+k_4)} \\ e^{ik_2} \\ e^{i(k_1+k_4)} \\ e^{i(k_2-k_3+k_4)} \\ 1 \\ e^{i(k_1-k_3+k_4)} \\ e^{i(k_2-k_3)} \\ e^{ik_1} \end{pmatrix} \psi_{p_5}. \quad (\text{B.11})$$

Defining the reduced vector $\tilde{\psi}$ as

$$\tilde{\psi} = (\psi_{p_5}; \psi_{C_5}, \dots, \psi_{C_8}; \psi_{\text{bulk}}), \quad (\text{B.12})$$

and using Eqs. (B.9) and (B.11), as well as an identity matrix for ψ_{bulk} , the matrix U can be easily constructed. Solving the generalized eigenvalue problem (B.7) numerically for each \mathbf{k} in the hyperbolic Brillouin zone, using standard linear algebra techniques, we obtain the hyperbolic bandstructure $\{E_n(\mathbf{k})\}$ and hyperbolic Bloch wavefunctions $\psi_{n\mathbf{k}}(x, y)$.

Appendix C: Point-group symmetries of the Bolza lattice

In ordinary crystallography, the group of all discrete symmetries of a Euclidean (periodic) lattice constitutes the space group \mathcal{G} . The translation group \mathcal{T} is an invariant or normal subgroup of \mathcal{G} ,

that is, if $h \in \mathcal{G}$, then $h\mathcal{T}h^{-1} = \mathcal{T}$. The point group \mathcal{P} is the factor group $\mathcal{P} \cong \mathcal{G}/\mathcal{T}$, i.e., space group operations with translations factored out [54]. Similarly, the group $G = \text{Aut}(X)$ of automorphisms of a compact Riemann surface $X \cong \mathbb{H}/\Gamma$ with Γ a co-compact, strictly hyperbolic Fuchsian group is isomorphic to the factor group [21]

$$G \cong N(\Gamma)/\Gamma, \quad (\text{C.1})$$

where $N(\Gamma)$ is the normalizer of Γ in $PSL(2, \mathbb{R})$ [55]:

$$N(\Gamma) = \{h \in PSL(2, \mathbb{R}) : h\Gamma h^{-1} = \Gamma\}. \quad (\text{C.2})$$

By analogy with Euclidean crystallography, it is natural to interpret $N(\Gamma)$ as a hyperbolic space group, its normal subgroup Γ as a (nonabelian) translation group, and the factor group (C.1) as a point group.

In this Appendix, we describe the group $G \cong \text{Aut}(\Sigma_2)$ of automorphisms of the Bolza surface (App. C1), interpreting it as a point group, and construct its linear action [Eq. (29)] on the Jacobian, i.e., hyperbolic \mathbf{k} -space (App. C2).

1. Automorphisms of the Bolza surface

The automorphism group G of the Bolza surface is a finite nonabelian group with 96 elements, of the form [39]

$$R^i S^j T^k U^l, \quad i = 0, \dots, 7, \quad j, k = 0, 1, \quad l = 0, 1, 2, \quad (\text{C.3})$$

where R, S, T, U are four generators. R and U are orientation-preserving hyperbolic isometries, i.e., Möbius transformations of the form (4). As discussed in Sec. II, and working in the Poincaré disk, the group Möb^+ of orientation-preserving Möbius transformations is isomorphic to $PSU(1, 1)$. S and T are reflections, and thus orientation-reversing isometries, which are again $PSU(1, 1)$ transformations, but of the form [43]

$$z \mapsto \gamma(z) = \frac{\alpha z^* + \beta}{\beta^* z^* + \alpha^*}, \quad (\text{C.4})$$

which is sometimes called an anti-Möbius or Möb^- transformation, and is the composition of an ordinary Möbius transformation with complex conjugation. Together, Möb^+ and Möb^- transformations form the general Möbius group, Möb , which is the full group $\text{Isom}(\mathbb{H})$ of isometries of the hyperbolic plane. In the next subsections we figure out the explicit form of the generators R, S, T, U of G as $PSU(1, 1)$ matrices. We first consider the Möb^+ generators R and U , then the Möb^- generators S and T .

Transformation R. The transformation R is a C_8 rotation $z \mapsto R(z) = e^{i2\pi/8}z$ about the center of the octagonal unit cell (Fig. C.1), which corresponds to the $SU(1, 1)$ matrix

$$R = \begin{pmatrix} e^{i\pi/8} & 0 \\ 0 & e^{-i\pi/8} \end{pmatrix}, \quad (\text{C.5})$$

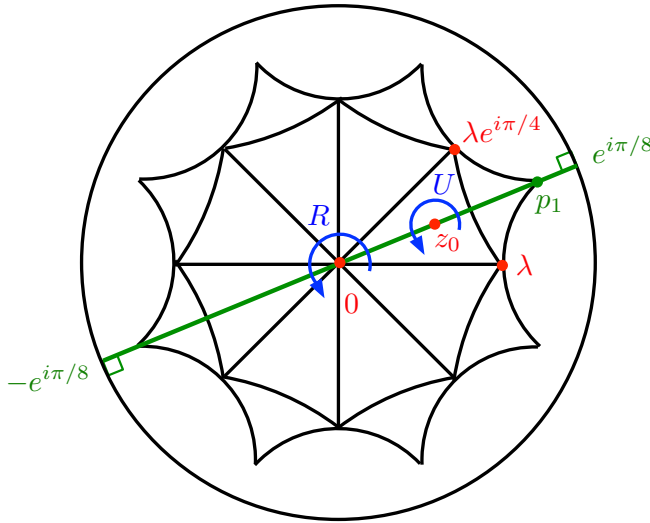


FIG. C.1. Automorphisms of the Bolza surface (adapted from Ref. [39]).

up to an overall sign.

Transformation U . This is a C_3 rotation around the center z_0 of a hyperbolic triangle, e.g., that formed by 0, λ , and $\lambda e^{i\pi/4}$ in Fig. C.1, where $\lambda = \sqrt{\sqrt{2}-1}$ (see Sec. III). The latter two vertices are found by considering that they are the midpoint of the boundary segments C_1 and C_2 , respectively, which corresponds to the point $\theta = \pi$ in the parametrization (18). The midpoints of C_1 and C_2 are thus $c - r$ and $e^{i\pi/4}(c - r)$, respectively, with c and r defined in Eq. (19), and $c - r = \lambda$.

We first need to find the center z_0 of that triangle. By symmetry, we expect z_0 to lie on the straight geodesic (green line in Fig. C.1) bisecting the triangle, i.e., $z_0 = ae^{i\pi/8}$ with $0 < a < \lambda$. We determine z_0 by requiring that it is the point of equal geodesic distance $d(z, z')$ from the three vertices of the triangle: $d(z_0, 0) = d(z_0, \lambda) = d(z_0, \lambda e^{i\pi/8})$. By symmetry, we see that the last equality is automatically satisfied, thus we only need to impose the first one to find a . The geodesic distance on the Poincaré disk is given by [43]

$$\cosh d(z, z') = 1 + \frac{2|z - z'|^2}{(1 - |z|^2)(1 - |z'|^2)}. \quad (\text{C.6})$$

Imposing the condition $d(z_0, z_1) = d(z_0, z_2)$ is thus the same as imposing

$$\frac{|z_0 - z_1|^2}{1 - |z_1|^2} = \frac{|z_0 - z_2|^2}{1 - |z_2|^2}. \quad (\text{C.7})$$

Setting $z_1 = 0$ and $z_2 = \lambda$, and after a bit of algebra, we obtain

$$a^2 - 2^{1/4}(1 + \sqrt{2})a + 1 = 0. \quad (\text{C.8})$$

Keeping the only root satisfying $0 < a < \lambda \approx 0.64$, we obtain

$$z_0 = \left(\frac{1 + \sqrt{2} - \sqrt{3}}{2^{3/4}} \right) e^{i\pi/8}. \quad (\text{C.9})$$

Now, U is a rotation by $2\pi/3$ around z_0 . We do not directly know what this looks like, but we know that a rotation around $z = 0$ is $C_3 : z \mapsto e^{i2\pi/3}z$. To obtain U , we simply have to “translate” (boost) z_0 to the origin, perform C_3 , then boost back to z_0 . In other words, $U = \gamma_\eta \circ C_3 \circ \gamma_\eta^{-1}$ where γ_η is a boost from $z = 0$ to $z = z_0$, i.e., along the green geodesic joining $-e^{i\pi/8}$ to $e^{i\pi/8}$. To find γ_η , first consider a boost $\tilde{\gamma}_\eta$ along the x axis. Such a boost by a quantity in $-\infty < \eta < \infty$ is given by [43]

$$\tilde{\gamma}_\eta : z \mapsto \tilde{\gamma}_\eta(z) = \frac{(\cosh \eta)z + \sinh \eta}{(\sinh \eta)z + \cosh \eta}, \quad (\text{C.10})$$

corresponding to a $PSU(1,1)$ transformation with $\alpha = \cosh \eta$, $\beta = \sinh \eta$. The fixed points of this transformation are the points at infinity ± 1 , and the origin is boosted to $\tilde{\gamma}_\eta(0) = \tanh \eta$. For $\eta > 0$ this is a boost towards the positive x axis. To boost along the green line, one should rotate down to the x axis, boost along the x axis, then rotate back to the green line. In other words, $\gamma_\eta = R_{\pi/8} \circ \tilde{\gamma}_\eta \circ R_{\pi/8}^{-1}$, where $R_{\pi/8} : z \mapsto e^{i\pi/8}z$ is a counterclockwise (C_{16}) rotation by $\pi/8$. We thus obtain

$$\gamma_\eta(z) = (R_{\pi/8} \circ \tilde{\gamma}_\eta \circ R_{\pi/8}^{-1})(z) = e^{i\pi/8} \left(\frac{(\cosh \eta)e^{-i\pi/8}z + \sinh \eta}{(\sinh \eta)e^{-i\pi/8}z + \cosh \eta} \right) = \frac{(\cosh \eta)z + e^{i\pi/8} \sinh \eta}{(e^{-i\pi/8} \sinh \eta)z + \cosh \eta}, \quad (\text{C.11})$$

a Möb⁺ transformation with $\alpha = \cosh \eta$, $\beta = e^{i\pi/8} \sinh \eta$. The points at infinity $\pm e^{i\pi/8}$ are fixed points of this transformation.

We now need to find the value of η such that $\gamma_\eta(0) = z_0$. This implies

$$\tanh \eta = \frac{1 + \sqrt{2} - \sqrt{3}}{2^{3/4}}. \quad (\text{C.12})$$

Writing $\sinh \eta = (1 + \sqrt{2} - \sqrt{3})b$ and $\cosh \eta = 2^{3/4}b$, and finding b using $\cosh^2 \eta - \sinh^2 \eta = 1$, we find that γ_η is a Möb⁺ transformation with

$$\alpha = \sqrt{\frac{\sqrt{3} + \sqrt{6} + 3}{6}} > 1, \quad \beta = e^{i\pi/8} \sqrt{\alpha^2 - 1}. \quad (\text{C.13})$$

Finally, to obtain U we conjugate C_3 by γ_η . In $SU(1,1)$ this is simply a product of matrices, and we find that U is a Möb⁺ transformation with

$$\alpha = e^{i3\pi/8} \sqrt{1 + \frac{1}{\sqrt{2}}}, \quad \beta = 2^{-1/4} e^{-i3\pi/8}. \quad (\text{C.14})$$

Transformation S. The transformation S is defined in Ref. [39] as a reflection across the green line in Fig. C.1. Define S' to be the reflection across the real axis, which sends $(x, y) \mapsto (x, -y)$ and is thus simply complex conjugation: $S' : z \mapsto z^*$, the simplest Möb⁻ transformation. A reflection S across the green line can be obtained by first rotating by $\pi/8$ clockwise to the real axis, performing S' , and then rotating back to the green line. We thus have:

$$S(z) = (R_{\pi/8} \circ S' \circ R_{\pi/8}^{-1})(z) = e^{i\pi/8}(e^{-i\pi/8}z)^* = e^{i2\pi/8}z^*, \quad (\text{C.15})$$

a transformation of the form (C.4) with $\alpha = e^{i\pi/8}$, $\beta = 0$.

Transformation T. According to Ref. [39], T is a Möb⁻ transformation which interchanges the origin $z = 0$ with a corner of the hyperbolic octagon, e.g., $p_1 = 2^{-1/4}e^{i\pi/8}$. Since it is a simple interchange, one should have $T^2 = e$ where e denotes the identity element in Möb⁺. (Note that the composition of two Möb⁻ transformations is in Möb⁺, and the composition of a Möb⁺ transformation and a Möb⁻ transformation is a Möb⁻ transformation.) Thus we have

$$T(z) = \frac{\alpha z^* + \beta}{\beta^* z^* + \alpha^*}, \quad (\text{C.16})$$

and wish to determine α and β . Imposing $T(0) = p_1$ implies $\beta = 2^{-1/4}e^{i\pi/8}\alpha^*$. Next, since $T^2 = e$ one has $T^2(0) = T(T(0)) = T(p_1) = 0$, which implies $\alpha e^{-i\pi/8} + \alpha^* e^{i\pi/8} = 0$. Since $\alpha \neq 0$, writing in polar form $\alpha = se^{i\theta}$, we find $\theta = 5\pi/8$. Finally, requiring that $|\alpha|^2 - |\beta|^2 = 1$, we find $s = 2^{1/4}\lambda^{-1} = \sqrt{2 + \sqrt{2}}$. Thus we find that T is a transformation of the form (C.4) with

$$\alpha = e^{i5\pi/8}\sqrt{2 + \sqrt{2}}, \quad \beta = e^{-i\pi/2}\sqrt{1 + \sqrt{2}}. \quad (\text{C.17})$$

Noting by explicit calculation that the composition $\gamma_1 \circ \gamma_2$ of two Möb⁻ transformations γ_1, γ_2 with $SU(1, 1)$ parameters α_1, β_1 and α_2, β_2 is a Möb⁺ transformation with $SU(1, 1)$ parameters α_{12}, β_{12} given by

$$\alpha_{12} = \alpha_1\alpha_2^* + \beta_1\beta_2, \quad \beta_{12} = \alpha_1\beta_2^* + \beta_1\alpha_2, \quad (\text{C.18})$$

we find that the $SU(1, 1)$ parameters of T^2 are $\alpha_{T^2} = |\alpha|^2 + \beta^2 = 1$ and $\beta_{T^2} = \alpha(\beta + \beta^*) = 0$, and thus $T^2 = e$.

Generator relations. According to Ref. [39], the automorphism group of the Bolza surface is finitely presented with relations

$$R^8 = S^2 = T^2 = U^3 = (RS)^2 = (ST)^2 = RTR^3T = e, \quad (\text{C.19})$$

$$UR = R^7U^2, \quad (\text{C.20})$$

$$U^2R = STU, \quad (\text{C.21})$$

$$US = SU^2, \quad (\text{C.22})$$

$$UT = RSU. \quad (\text{C.23})$$

Using the explicit form of the generators just derived, we verify that all relations hold as identities in Möb, except $RT R^3 T = e$. We find

$$RT R^3 T = \gamma_3 \gamma_4^{-1} \gamma_1^{-1} \in \Gamma, \quad (\text{C.24})$$

where $\gamma_1, \gamma_2, \gamma_3, \gamma_4$ are the Fuchsian group generators (21), thus $RT R^3 T$ indeed reduces to the identity in $G = \text{Aut}(\Sigma_2) \cong N(\Gamma)/\Gamma$. Similarly, Ref. [39] states that $Z(G)$, the center of G (i.e., the set of elements that commute with every element of G), is isomorphic to \mathbb{Z}_2 and generated by $R^4 : z \mapsto -z$. To verify this, it is sufficient to verify that R^4 commutes with S, T, U . Commutation with S holds as an identity in Möb, while for the remaining two generators we find

$$\gamma_1 R^4 U = U R^4, \quad \gamma_1 \gamma_4 \gamma_3^{-1} \gamma_2 R^4 T = T R^4, \quad (\text{C.25})$$

which indeed reduce to $R^4 U = U R^4$ and $R^4 T = T R^4$ in the quotient $G \cong N(\Gamma)/\Gamma$.

2. Point-group action on hyperbolic k -space

In the previous section, we explicitly constructed the action of the point group G in real space. In this section, we determine how G acts in four-dimensional \mathbf{k} -space, via its action on the automorphic Bloch eigenstates.

Given a general (orientation-preserving or -reversing) transformation $\gamma \in \text{Möb}$, define a linear operator \mathcal{S}_γ which performs the corresponding transformation on a wavefunction $\psi(x, y) = \psi(z)$:

$$\mathcal{S}_\gamma \psi(z) \equiv \psi(\gamma(z)). \quad (\text{C.26})$$

For the derivation that follows, it will be useful to treat z and z^* as independent “real” variables, and the transformation (C.26) will be written as $\mathcal{S}_\gamma \psi(z, z^*) = \psi(\gamma(z), \gamma(z)^*)$.

Point-group symmetry of the Hamiltonian. We assume the potential V is not only automorphic with respect to the Fuchsian group Γ of hyperbolic lattice translations, but also invariant under point-group transformations,

$$\mathcal{S}_h V(z, z^*) \mathcal{S}_h^{-1} = V(h(z), h(z)^*) = V(z, z^*), \quad \forall h \in G \subset \text{Möb}. \quad (\text{C.27})$$

In other words, $[\mathcal{S}_h, V] = 0$ for all $h \in G$. We also want to show the kinetic term $H_0 = -\Delta$ commutes with \mathcal{S}_h , where

$$\Delta = (1 - zz^*)^2 \frac{\partial^2}{\partial z \partial z^*}, \quad (\text{C.28})$$

is the hyperbolic Laplacian (6), where we have used $\partial_x = \partial_z + \partial_{z^*}$ and $\partial_y = i(\partial_z - \partial_{z^*})$. We can in fact show that Δ is invariant under the action of any $\gamma \in \text{Möb}$. First, Δ is obviously invariant under complex conjugation $z \mapsto z^*$. Since any Möb[−] transformation can be written as

the composition of a Möb⁺ transformation with complex conjugation, it is sufficient to show that Δ is invariant under Möb⁺ transformations. Consider an arbitrary Möb⁺ transformation,

$$z \mapsto w \equiv \gamma(z) = \frac{\alpha z + \beta}{\beta^* z + \alpha^*}, \quad z^* \mapsto w^* \equiv \gamma(z)^* = \frac{\alpha^* z^* + \beta^*}{\beta z^* + \alpha}. \quad (\text{C.29})$$

We have

$$\begin{aligned} (\Delta \mathcal{S}_\gamma) \psi(z, z^*) &= (1 - zz^*)^2 \frac{\partial^2}{\partial z \partial z^*} \psi(w, w^*) \\ &= (1 - zz^*)^2 \frac{\partial w}{\partial z} \frac{\partial w^*}{\partial z^*} \frac{\partial^2}{\partial w \partial w^*} \psi(w, w^*) \\ &= (1 - zz^*)^2 \left| \frac{\partial w}{\partial z} \right|^2 \frac{\partial^2}{\partial w \partial w^*} \psi(w, w^*). \end{aligned} \quad (\text{C.30})$$

On the other hand, we have

$$(\mathcal{S}_\gamma \Delta) \psi(z, z^*) = \mathcal{S}_\gamma \left((1 - zz^*)^2 \frac{\partial^2}{\partial z \partial z^*} \psi(z, z^*) \right) = (1 - ww^*)^2 \frac{\partial^2}{\partial w \partial w^*} \psi(w, w^*). \quad (\text{C.31})$$

Using (C.29), we have

$$1 - ww^* = \frac{1 - zz^*}{|\beta^* z + \alpha^*|^2}. \quad (\text{C.32})$$

On the other hand, we have

$$\frac{\partial w}{\partial z} = \frac{1}{(\beta^* z + \alpha^*)^2}, \quad (\text{C.33})$$

thus $[\mathcal{S}_\gamma, \Delta] = 0$ for any $\gamma \in \text{Möb}$, and in particular for $\gamma \in G$. As a result, $[\mathcal{S}_h, H] = 0$ for any $h \in G$, with $H = -\Delta + V$ the full Hamiltonian.

Point-group symmetry of hyperbolic Bloch eigenstates. We now go back to treating $z = x + iy \in \mathbb{C}$ as a complex coordinate in the Poincaré disk. Consider an eigenstate $\psi_{\mathbf{k}}(z)$ of H with energy $E(\mathbf{k})$, that obeys the four automorphic Bloch conditions (25):

$$\psi_{\mathbf{k}}(\gamma_j(z)) = e^{ik_j} \psi_{\mathbf{k}}(z), \quad j = 1, \dots, 4. \quad (\text{C.34})$$

with $\gamma_1, \dots, \gamma_4$ in Eq. (21). Since \mathcal{S}_h with $h \in G$ commutes with H , the state

$$\psi_{\mathbf{k}}^h(z) \equiv \mathcal{S}_h \psi_{\mathbf{k}}(z) = \psi_{\mathbf{k}}(h(z)), \quad (\text{C.35})$$

for a given $h \in G$ is also an eigenstate of H with the same eigenenergy $E(\mathbf{k})$. However, it does not in general obey the same Bloch conditions as $\psi_{\mathbf{k}}(z)$. Indeed, first write Eq. (C.34) as

$$\mathcal{S}_{\gamma_j} \psi_{\mathbf{k}}(z) = e^{ik_j} \psi_{\mathbf{k}}(z), \quad j = 1, \dots, 4. \quad (\text{C.36})$$

	γ_1	γ_2	γ_3	γ_4
R	γ_2	γ_3	γ_4	γ_1^{-1}
S	γ_2	γ_1	γ_4^{-1}	γ_3^{-1}
T	$\gamma_4^{-1}\gamma_3\gamma_2^{-1}$	$\gamma_3\gamma_4^{-1}\gamma_1^{-1}$	$\gamma_2\gamma_4^{-1}\gamma_1^{-1}$	$\gamma_2\gamma_3^{-1}\gamma_1^{-1}$
U	$\gamma_2\gamma_1^{-1}$	γ_1^{-1}	$\gamma_4^{-1}\gamma_1^{-1}$	$\gamma_4^{-1}\gamma_3\gamma_2^{-1}$

TABLE I. Conjugation of Fuchsian group generators by point-group symmetries.

Acting with \mathcal{S}_h on both sides and inserting the identity in the form $\mathcal{S}_h^{-1}\mathcal{S}_h = \mathbb{I}$, where the defining action of the inverse operator is

$$\mathcal{S}_\gamma^{-1}\psi(z) = \psi(\gamma^{-1}(z)), \quad \gamma \in \text{Möb}, \quad (\text{C.37})$$

and \mathbb{I} is the identity operator, we have

$$\mathcal{S}_h\mathcal{S}_{\gamma_j}\mathcal{S}_h^{-1}\psi_{\mathbf{k}}^h(z) = e^{ik_j}\psi_{\mathbf{k}}^h(z), \quad j = 1, \dots, 4. \quad (\text{C.38})$$

In other words, $\psi_{\mathbf{k}}^h$ obeys the modified Bloch conditions

$$\psi_{\mathbf{k}}^h((h\gamma_j h^{-1})(z)) = e^{ik_j}\psi_{\mathbf{k}}^h(z), \quad j = 1, \dots, 4. \quad (\text{C.39})$$

The modified boundary conditions (C.39) involve the conjugation of the Fuchsian group generator $\gamma_j \in \Gamma$ by point-group elements $h \in G$. Given Eqs. (C.1-C.2), $h\gamma_j h^{-1}$ is again necessarily in Γ . (Although h can be either in Möb^+ or Möb^- , $h\gamma_j h^{-1}$ is necessarily in Möb^+ , since the inverse of an element of Möb^- is also in Möb^- , and only an even number (which could be zero) of Möb^- transformations appear in $h\gamma_j h^{-1}$. Therefore the boundary conditions obeyed by $\psi_{\mathbf{k}}^h$ preserve orientation, as those for $\psi_{\mathbf{k}}$.) From the explicit forms of the four generators $h = R, S, T, U$ of G , determined earlier, and the four generators γ_j in Eq. (21), we can compute $h\gamma_j h^{-1}$. We display the result of these computations in Table I, with $h \in \{R, S, T, U\}$ as the row index and $\gamma_j \in \{\gamma_1, \gamma_2, \gamma_3, \gamma_4\}$ as the column index. These expressions in terms of the γ_j are not unique, since one can use the relation (23) to obtain different (but equivalent) expressions. Furthermore, since $h\gamma_j^{-1}h^{-1} = (h\gamma_j h^{-1})^{-1}$, the conjugated inverse generators $h\gamma_j^{-1}h^{-1}$ are easily determined from Table I as well.

Using the results above, we can now show that $\psi_{\mathbf{k}}^h$ corresponds to a hyperbolic Bloch eigenstate with a transformed wavevector \mathbf{k}^h , i.e.,

$$\psi_{\mathbf{k}}^h(\gamma_j(z)) = e^{ik_j^h}\psi_{\mathbf{k}}^h(z), \quad j = 1, \dots, 4. \quad (\text{C.40})$$

To show this, we first observe that for a given point-group generator h , the relations in Table I can be inverted to express any original generator γ_j in terms of the conjugated generators $\gamma_j^h \equiv h\gamma_j h^{-1}$.

We find

$$\gamma_1 = (\gamma_4^R)^{-1} = \gamma_2^S = (\gamma_4^T)^{-1} \gamma_3^T (\gamma_2^T)^{-1} = (\gamma_2^U)^{-1}, \quad (\text{C.41})$$

$$\gamma_2 = \gamma_1^R = \gamma_1^S = \gamma_3^T (\gamma_4^T)^{-1} (\gamma_1^T)^{-1} = \gamma_1^U (\gamma_2^U)^{-1}, \quad (\text{C.42})$$

$$\gamma_3 = \gamma_2^R = (\gamma_4^S)^{-1} = \gamma_2^T (\gamma_4^T)^{-1} (\gamma_1^T)^{-1} = \gamma_1^U \gamma_4^U (\gamma_3^U)^{-1}, \quad (\text{C.43})$$

$$\gamma_4 = \gamma_3^R = (\gamma_3^S)^{-1} = \gamma_2^T (\gamma_3^T)^{-1} (\gamma_1^T)^{-1} = \gamma_2^U (\gamma_3^U)^{-1}. \quad (\text{C.44})$$

Writing Eq. (C.39) as

$$\psi_{\mathbf{k}}^h(\gamma_j^h(z)) = e^{ik_j} \psi_{\mathbf{k}}^h(z), \quad j = 1, \dots, 4, \quad (\text{C.45})$$

we have, taking $h = R$,

$$\psi_{\mathbf{k}}^R(\gamma_1(z)) = \psi_{\mathbf{k}}^R((\gamma_4^R)^{-1}(z)) = e^{-ik_4} \psi_{\mathbf{k}}^R(z), \quad (\text{C.46})$$

$$\psi_{\mathbf{k}}^R(\gamma_2(z)) = \psi_{\mathbf{k}}^R(\gamma_1^R(z)) = e^{ik_1} \psi_{\mathbf{k}}^R(z), \quad (\text{C.47})$$

$$\psi_{\mathbf{k}}^R(\gamma_3(z)) = \psi_{\mathbf{k}}^R(\gamma_2^R(z)) = e^{ik_2} \psi_{\mathbf{k}}^R(z), \quad (\text{C.48})$$

$$\psi_{\mathbf{k}}^R(\gamma_4(z)) = \psi_{\mathbf{k}}^R(\gamma_3^R(z)) = e^{ik_3} \psi_{\mathbf{k}}^R(z), \quad (\text{C.49})$$

where in Eq. (C.46) we have used the relation $\psi_{\mathbf{k}}^h((\gamma_j^h)^{-1}(z)) = e^{-ik_j} \psi_{\mathbf{k}}^h(z)$, $j = 1, \dots, 4$, easily shown by substituting $z \rightarrow (\gamma_j^h)^{-1}(z)$ in Eq. (C.45). Thus Eqs. (C.46-C.49) can be written as Eq. (C.40) with

$$\mathbf{k}^R = (k_1^R, k_2^R, k_3^R, k_4^R) = (-k_4, k_1, k_2, k_3). \quad (\text{C.50})$$

Proceeding similarly for $h = S, T, U$, we find that the $\psi_{\mathbf{k}}^h$ obey Eq. (C.40) with

$$\mathbf{k}^S = (k_1^S, k_2^S, k_3^S, k_4^S) = (k_2, k_1, -k_4, -k_3), \quad (\text{C.51})$$

$$\mathbf{k}^T = (k_1^T, k_2^T, k_3^T, k_4^T) = (-k_2 + k_3 - k_4, -k_1 + k_3 - k_4, -k_1 + k_2 - k_4, -k_1 + k_2 - k_3), \quad (\text{C.52})$$

$$\mathbf{k}^U = (k_1^U, k_2^U, k_3^U, k_4^U) = (-k_2, k_1 - k_2, k_1 - k_3 + k_4, k_2 - k_3). \quad (\text{C.53})$$

The linear relations (C.50-C.53) can be written in the matrix form of Eq. (29) in the main text,

$$k_i^h = M_{ij}(h) k_j, \quad (\text{C.54})$$

with the 4×4 matrices:

$$\begin{aligned} M(R) &= \begin{pmatrix} 0 & 0 & 0 & -1 \\ 1 & 0 & 0 & 0 \\ 0 & 1 & 0 & 0 \\ 0 & 0 & 1 & 0 \end{pmatrix}, & M(S) &= \begin{pmatrix} 0 & 1 & 0 & 0 \\ 1 & 0 & 0 & 0 \\ 0 & 0 & 0 & -1 \\ 0 & 0 & -1 & 0 \end{pmatrix}, \\ M(T) &= \begin{pmatrix} 0 & -1 & 1 & -1 \\ -1 & 0 & 1 & -1 \\ -1 & 1 & 0 & -1 \\ -1 & 1 & -1 & 0 \end{pmatrix}, & M(U) &= \begin{pmatrix} 0 & -1 & 0 & 0 \\ 1 & -1 & 0 & 0 \\ 1 & 0 & -1 & 1 \\ 0 & 1 & -1 & 0 \end{pmatrix}. \end{aligned} \quad (\text{C.55})$$

Equation (C.54) can be thought of as the genus-2 analog of the Euclidean relation $k_i^h = h_{ij}k_j$, that follows from straightforward Fourier analysis, where $h \in G \subset O(2)$ is a Euclidean point-group transformation $r_i \rightarrow h_{ij}r_j$ in real space. In fact, we find that the matrices (C.55) form a linear representation of the automorphism group G of the Bolza surface in four-dimensional hyperbolic \mathbf{k} -space, in the sense that those matrices obey the group relations (C.19-C.23), with $M(h_1h_2) = M(h_1)M(h_2)$ for $h_1, h_2 \in G$, and $M(e)$ is the 4×4 identity matrix.

Appendix D: Hyperbolic Wannier functions

In this last Appendix we show that the hyperbolic Wannier functions (36) are orthonormal and derive their automorphic transformation property (37). We perform the derivation in genus 2, but it can be straightforwardly generalized to higher genus. The inner product of two hyperbolic Wannier functions is:

$$\int_{\mathbb{H}} d^2z \sqrt{g} f_n^*(\mathbf{R}, z) f_{n'}(\mathbf{R}', z) = \int_{\text{Jac}(\Sigma_2)} \frac{d^4k}{(2\pi)^4} \int_{\text{Jac}(\Sigma_2)} \frac{d^4k'}{(2\pi)^4} e^{i\mathbf{k} \cdot \mathbf{R}} e^{-i\mathbf{k}' \cdot \mathbf{R}'} \int_{\mathbb{H}} d^2z \sqrt{g} \psi_{n\mathbf{k}}^*(z) \psi_{n'\mathbf{k}'}(z). \quad (\text{D.1})$$

For $\mathbf{k} \neq \mathbf{k}'$, the hyperbolic Bloch eigenstates $\psi_{n\mathbf{k}}(z)$ and $\psi_{n'\mathbf{k}'}(z)$, as constructed in our work, obey different boundary conditions and thus formally live in different Hilbert spaces; we cannot directly invoke their orthogonality. To circumvent this problem, we use the invariance of the integration measure $d^2z \sqrt{g}$ under Möbius transformations and the fact that \mathcal{D} is a fundamental region for Γ to write

$$\mathbb{H} = \bigcup_{\gamma \in \Gamma} \gamma(\mathcal{D}), \quad (\text{D.2})$$

and thus

$$\begin{aligned} \int_{\mathbb{H}} d^2z \sqrt{g} \psi_{n\mathbf{k}}^*(z) \psi_{n'\mathbf{k}'}(z) &= \sum_{\gamma \in \Gamma} \int_{\mathcal{D}} d^2z \sqrt{g} \psi_{n\mathbf{k}}^*(\gamma(z)) \psi_{n'\mathbf{k}'}(\gamma(z)) \\ &= \sum_{\gamma \in \Gamma} \chi_{\mathbf{k}}^*(\gamma) \chi_{\mathbf{k}'}(\gamma) \int_{\mathcal{D}} d^2z \sqrt{g} \psi_{n\mathbf{k}}^*(z) \psi_{n'\mathbf{k}'}(z), \end{aligned} \quad (\text{D.3})$$

using the Bloch condition (13). Despite the fact that Γ is discrete but not finite (and hence only locally compact), the Bloch phase factors $\chi_{\mathbf{k}}$ obey a Schur-type orthogonality relation that can be derived as follows. Define $M = \sum_{\gamma \in \Gamma} \chi_{\mathbf{k}}^*(\gamma) \chi_{\mathbf{k}'}(\gamma)$. For $\mathbf{k} = \mathbf{k}'$, M is clearly infinite. For $\mathbf{k} \neq \mathbf{k}'$, multiply M by $\chi_{\mathbf{k}}(\gamma')$ for an arbitrary $\gamma' \neq e$ in Γ :

$$\chi_{\mathbf{k}}(\gamma') M = \sum_{\gamma \in \Gamma} \chi_{\mathbf{k}}(\gamma') \chi_{\mathbf{k}}(\gamma^{-1}) \chi_{\mathbf{k}'}(\gamma) \chi_{\mathbf{k}'}(\gamma'^{-1}) \chi_{\mathbf{k}'}(\gamma') = \sum_{\gamma \in \Gamma} \chi_{\mathbf{k}}^*(\gamma \gamma'^{-1}) \chi_{\mathbf{k}'}(\gamma \gamma'^{-1}) \chi_{\mathbf{k}'}(\gamma'). \quad (\text{D.4})$$

Replacing $\gamma \rightarrow \gamma\gamma'$ in the last sum, we find $\chi_{\mathbf{k}}(\gamma')M = M\chi_{\mathbf{k}'}(\gamma')$ for arbitrary $\gamma' \in \Gamma$. But since $\mathbf{k} \neq \mathbf{k}'$, $\chi_{\mathbf{k}}(\gamma') \neq \chi_{\mathbf{k}'}(\gamma')$, and thus $M = 0$. Since $\mathbf{k}, \mathbf{k}' \in \text{Jac}(\Sigma_2)$ are continuous, we must have

$$\sum_{\gamma \in \Gamma} \chi_{\mathbf{k}}^*(\gamma) \chi_{\mathbf{k}'}(\gamma) = A\delta(\mathbf{k} - \mathbf{k}'), \quad (\text{D.5})$$

for some constant A . Substituting into Eq. (D.3), we have

$$\int_{\mathbb{H}} d^2z \sqrt{g} \psi_{n\mathbf{k}}^*(z) \psi_{n'\mathbf{k}'}(z) = A\delta(\mathbf{k} - \mathbf{k}') \int_{\mathcal{D}} d^2z \sqrt{g} \psi_{n\mathbf{k}}^*(z) \psi_{n'\mathbf{k}}(z) = (2\pi)^4 \delta(\mathbf{k} - \mathbf{k}') \delta_{nn'}, \quad (\text{D.6})$$

using the orthogonality of hyperbolic Bloch eigenstates on \mathcal{D} with the same \mathbf{k} , and normalizing those eigenstates so as to absorb the constant A . Substituting in Eq. (D.1), we find that the hyperbolic Wannier functions for different bands n, n' and on different sites $\mathbf{R} \in \mathbb{Z}^4$ are orthonormal:

$$\int_{\mathbb{H}} d^2z \sqrt{g} f_n^*(\mathbf{R}, z) f_{n'}(\mathbf{R}', z) = \delta_{nn'} \delta_{\mathbf{R}\mathbf{R}'}. \quad (\text{D.7})$$

Finally, the automorphic transformation property (37) of hyperbolic Wannier functions is easily established from their definition (36). For the Fuchsian translation $\gamma_{\mathbf{m}} = \gamma_1^{m_1} \gamma_2^{m_2} \gamma_3^{m_3} \gamma_4^{m_4}$ and $\mathbf{m} = (m_1, m_2, m_3, m_4) \in \mathbb{Z}^4$, we have:

$$\begin{aligned} f_n(\mathbf{R} + \mathbf{m}, \gamma_{\mathbf{m}}(z)) &= \int_{\text{Jac}(\Sigma_2)} \frac{d^4k}{(2\pi)^4} e^{-i\mathbf{k} \cdot (\mathbf{R} + \mathbf{m})} \psi_{n\mathbf{k}}(\gamma_{\mathbf{m}}(z)) \\ &= \int_{\text{Jac}(\Sigma_2)} \frac{d^4k}{(2\pi)^4} e^{-i\mathbf{k} \cdot \mathbf{R}} e^{-i\mathbf{k} \cdot \mathbf{m}} \chi_{\mathbf{k}}(\gamma_{\mathbf{m}}) \psi_{n\mathbf{k}}(z) \\ &= f_n(\mathbf{R}, z), \end{aligned} \quad (\text{D.8})$$

where in the last line we used the fact that $\chi_{\mathbf{k}}(\gamma_{\mathbf{m}}) = e^{i\mathbf{k} \cdot \mathbf{m}}$. This makes clear the fact that Eq. (37) holds for any $\gamma_{\mathbf{m}}$ which obeys this latter property.

-
- [1] F. Bloch, “Über die Quantenmechanik der Elektronen in Kristallgittern,” *Z. Phys.* **52**, 555–600 (1929).
 - [2] While our discussion is applicable to wave phenomena in general, for concreteness we will utilize the language of quantum condensed matter physics and employ a units convention familiar in that field, whereas the reduced Planck’s constant \hbar is set to one, and the terms “momentum” and “wave vector”, and “energy” and “frequency”, are used interchangeably.
 - [3] N. W. Ashcroft and N. D. Mermin, *Solid State Physics* (Saunders College, Philadelphia, 1976).
 - [4] F. D. M. Haldane, “Model for a quantum Hall effect without Landau levels: condensed-matter realization of the ‘parity anomaly’,” *Phys. Rev. Lett.* **61**, 2015–2018 (1988).
 - [5] For a recent review, see, e.g., C.-K. Chiu, J. C. Y. Teo, A. P. Schnyder, and S. Ryu, “Classification of topological quantum matter with symmetries”, *Rev. Mod. Phys.* **88**, 035005 (2016).

- [6] P. J. Steinhardt and S. Ostlund, *The Physics of Quasicrystals* (World Scientific, Singapore, 1987).
- [7] T. Janssen and A. Janner, “Aperiodic crystals and superspace concepts,” [Acta Crystallogr. Sect. B **70**, 617–651 \(2014\)](#).
- [8] A. J. Kollár, M. Fitzpatrick, and A. A. Houck, “Hyperbolic lattices in circuit quantum electrodynamics,” [Nature **571**, 45–50 \(2019\)](#).
- [9] H. S. M. Coxeter, “Crystal symmetry and its generalizations,” *Trans. Royal Soc. Canada* **51**, 1–13 (1957).
- [10] H. S. M. Coxeter, “The non-Euclidean symmetry of Escher’s picture ‘Circle Limit III’,” [Leonardo **12**, 19–25 \(1979\)](#).
- [11] A. J. Kollár, M. Fitzpatrick, P. Sarnak, and A. A. Houck, “Line-graph lattices: Euclidean and non-Euclidean flat bands, and implementations in circuit quantum electrodynamics,” [Commun. Math. Phys. \(2019\)](#), [10.1007/s00220-019-03645-8](#).
- [12] I. Boettcher, P. Bienias, R. Belyansky, A. J. Kollár, and A. V. Gorshkov, “Quantum simulation of hyperbolic space with circuit quantum electrodynamics: from graphs to geometry,” [arXiv:1910.12318 \(2019\)](#).
- [13] S. Yu, X. Piao, and N. Park, “Topological hyperbolic lattices,” [Phys. Rev. Lett. **125**, 053901 \(2020\)](#).
- [14] D. Mumford, *Tata Lectures on Theta I* (Birkhäuser, Boston, 1983).
- [15] S. Katok, *Fuchsian Groups* (The University of Chicago Press, Chicago, 1992).
- [16] X. G. Wen, “Vacuum degeneracy of chiral spin states in compactified space,” [Phys. Rev. B **40**, 7387 \(1989\)](#).
- [17] A. B. Venkov, *Spectral Theory of Automorphic Functions and Its Applications* (Kluwer Academic Publishers, Dordrecht, 1990).
- [18] The key aspects of hyperbolic geometry we will be needing here, such as the Poincaré disk model, the compactification of the hyperbolic octagon, and the hyperbolic Laplacian, are reviewed in a language accessible to scientists in Ref. [43].
- [19] M. Nakahara, *Geometry, Topology, and Physics* (IOP Publishing, Bristol, 1990).
- [20] J. H. Silverman, “Elliptic curves and cryptography,” [Proc. Sympos. Appl. Math. **62**, 91–112 \(2005\)](#).
- [21] H. M. Farkas and I. Kra, *Riemann Surfaces*, 2nd ed. (Springer, New York, 1992).
- [22] R. C. Gunning, “The structure of factors of automorphy,” [Amer. J. Math. **78**, 357–382 \(1956\)](#).
- [23] D. A. Hejhal, *The Selberg Trace Formula for $PSL(2, \mathbb{R})$* , Vol. 1 (Springer-Verlag, Berlin, 1976).
- [24] A. Newlander and L. Nirenberg, “Complex analytic coordinates in almost complex manifolds,” [Ann. of Math. **65**, 391–404 \(1957\)](#).
- [25] G. Kiremidjian, “Complex structures on Riemann surfaces,” [Trans. Amer. Math. Soc. **169**, 317–336 \(1972\)](#).
- [26] D. Huybrechts, *Complex Geometry* (Springer-Verlag, Berlin, 2005).
- [27] O. Forster, *Lectures on Riemann Surfaces* (Springer-Verlag, New York-Berlin, 1981).
- [28] R. Miranda, *Algebraic Curves and Riemann Surfaces* (American Mathematical Society, Providence,

1995).

- [29] I. G. Macdonald, “Symmetric products of an algebraic curve,” [Topology](#) **1**, 319–343 (1962).
- [30] H. Ninnemann, “Gutzwiller’s octagon and the triangular billiard $T^*(2, 3, 8)$ as models for the quantization of chaotic systems by Selberg’s trace formula,” [Int. J. Mod. Phys. B](#) **09**, 1647–1753 (1995).
- [31] O. Bolza, “On binary sextics with linear transformations into themselves,” [Am. J. Math.](#) **10**, 47–70 (1887).
- [32] P. Deligne and D. Mumford, “The irreducibility of the space of curves of given genus,” [Inst. Hautes Études Sci. Publ. Math.](#) **36**, 75–109 (1969).
- [33] A. Strohmaier and V. Uski, “An algorithm for the computation of eigenvalues, spectral zeta functions and zeta-determinants on hyperbolic surfaces,” [Commun. Math. Phys.](#) **317**, 827–869 (2013).
- [34] P. Buser, *Geometry and Spectra of Compact Riemann Surfaces* (Birkhäuser, Boston, 1992).
- [35] R. Aurich and F. Steiner, “Periodic-orbit sum rules for the Hadamard-Gutzwiller model,” [Physica D](#) **39**, 169–193 (1989).
- [36] R. Aurich and F. Steiner, “Statistical properties of highly excited quantum eigenstates of a strongly chaotic system,” [Physica D](#) **64**, 185–214 (1993).
- [37] A. Bachelot-Motet, “Wave computation on the hyperbolic double doughnut,” [J. Comput. Math.](#) **28**, 790–806 (2010).
- [38] F. Hecht, “New development in freefem++,” [J. Numer. Math.](#) **20**, 251–266 (2012).
- [39] J. Cook, *Properties of Eigenvalues on Riemann Surfaces with Large Symmetry Groups*, Ph.D. thesis, Loughborough University (2018).
- [40] J. von Neumann and E. P. Wigner, “Über das Verhalten von Eigenwerten bei adiabatischen Prozessen,” [Z. Phys.](#) **30**, 467–470 (1929).
- [41] C. Fang, H. Weng, X. Dai, and Z. Fang, “Topological nodal line semimetals,” [Chinese Phys. B](#) **25**, 117106 (2016).
- [42] R. Donagi, “Spectral covers,” in *Current Topics in Complex Algebraic Geometry (Berkeley, CA, 1992/93)*, Math. Sci. Res. Inst. Publ., Vol. 28 (Cambridge Univ. Press, Cambridge, 1995) pp. 65–86.
- [43] N. L. Balazs and A. Voros, “Chaos on the pseudosphere,” [Phys. Rep.](#) **143**, 109–240 (1986).
- [44] J. F. Cariñena, M. F. Rañada, and M. Santander, “The quantum harmonic oscillator on the sphere and the hyperbolic plane,” [Ann. Phys. \(N.Y.\)](#) **322**, 2249–2278 (2007).
- [45] A. Selberg, “Harmonic analysis and discontinuous groups in weakly symmetric Riemannian spaces with applications to Dirichlet series,” [J. Indian Math. Soc.](#) **20**, 47–87 (1956).
- [46] R. Laza, M. Schütt, and N. Yui, eds., *Arithmetic and Geometry of K3 Surfaces and Calabi-Yau Threefolds*, Proceedings of the Workshop Held at the Fields Institute and University of Toronto, Toronto, ON, August 16–25, 2011, Fields Institute Communications, Vol. 67 (Springer, New York; Fields Institute for Research in Mathematical Sciences, Toronto, ON, 2013).
- [47] P. Deligne, J. S. Milne, A. Ogus, and K.-Y. Shih, *Hodge Cycles, Motives, and Shimura Varieties* (Springer-Verlag, Berlin-New York, 1982).

- [48] K. Hori, S. Katz, A. Klemm, R. Pandharipande, R. P. Thomas, C. Vafa, R. Vakil, and E. Zaslow, *Mirror Symmetry* (American Mathematical Society, Providence, RI; Clay Mathematics Institute, Cambridge, MA, 2003).
- [49] W. P. Thurston, “Three dimensional manifolds, Kleinian groups and hyperbolic geometry,” [Bull. Amer. Math. Soc. \(N.S.\)](#) **6**, 357–381 (1982).
- [50] S. K. Donaldson and R. P. Thomas, “Gauge theory in higher dimensions,” in *The Geometric Universe (Oxford, 1996)* (Oxford Univ. Press, Oxford, 1998) pp. 31–47.
- [51] A.-C. Hladky-Hennion and J.-N. Decarpigny, “Analysis of the scattering of a plane acoustic wave by a doubly periodic structure using the finite element method: Application to Alberich anechoic coatings,” [J. Acoust. Soc. Am.](#) **90**, 3356–3367 (1991).
- [52] P. Langlet, A.-C. Hladky-Hennion, and J.-N. Decarpigny, “Analysis of the propagation of plane acoustic waves in passive periodic materials using the finite element method,” [J. Acoust. Soc. Am.](#) **98**, 2792–2800 (1995).
- [53] S. Ballandras, M. Wilm, P.-F. Edoa, A. Soufyane, V. Laude, W. Steichen, and R. Lardat, “Finite-element analysis of periodic piezoelectric transducers,” [J. Appl. Phys.](#) **93**, 702–711 (2002).
- [54] R. L. Liboff, *Primer for Point and Space Groups* (Springer-Verlag, New York, 2004).
- [55] In Riemann surface theory [21], one is typically interested in orientation-preserving automorphisms, thus $N(\Gamma)$ is defined as the normalizer of Γ in $\text{Möb}^+ \cong PSL(2, \mathbb{R})$, the group of orientation-preserving Möbius transformations. Here we consider all automorphisms [39], both Möb^+ and orientation-reversing ones (Möb^-), and $N(\Gamma)$ is more properly defined as the normalizer of Γ in the general Möbius group Möb .